

# Double white dwarf mergers and elemental surface abundances in extreme helium and R Coronae Borealis stars

C.S.Jeffery<sup>1,2\*</sup>, A.I.Karakas<sup>3†</sup> & H.Saio<sup>4‡</sup>

<sup>1</sup>*Armagh Observatory, College Hill, Armagh BT61 9DG, Northern Ireland*

<sup>2</sup>*School of Physics, Trinity College Dublin, Dublin 2, Ireland*

<sup>3</sup>*Research School of Astronomy & Astrophysics, Mt Stromlo Observatory, Canberra, Australia*

<sup>4</sup>*Astronomical Institute, School of Science, Tohoku University, Sendai 980-8578, Japan*

Accepted ..... Received ..... ; in original form .....

## ABSTRACT

The surface abundances of extreme helium (EHe) and R Coronae Borealis (RCB) stars are discussed in terms of a model for their origin in the merger of a carbon-oxygen white dwarf with a helium white dwarf. The model is expressed as a linear mixture of the individual layers of both constituent white dwarfs, taking account of the specific evolution of each star. In developing this recipe from previous versions, particular attention has been given to the inter-shell abundances of the asymptotic giant branch star which evolved to become the carbon-oxygen white dwarf. Thus the surface composition of the merged star is estimated as a function of the initial mass and metallicity of its progenitor. The question of whether additional nucleosynthesis occurs during the white dwarf merger has been examined by including the results of recent hydrodynamical merger calculations which incorporate the major nuclear networks.

The high observed abundances of carbon and oxygen must either originate by dredge-up from the core of the carbon-oxygen white dwarf during a *cold* merger or be generated directly by  $\alpha$ -burning during a *hot* merger. The presence of large quantities of  $^{18}\text{O}$  may be consistent with both scenarios, since a significant  $^{18}\text{O}$  pocket develops at the carbon/helium boundary in a number of our post-AGB models.

The production of fluorine, neon and phosphorus in the AGB intershell propagates through to an overabundance at the surface of the merged stars, but generally not in sufficient quantity to match the observed abundances. However, the evidence for an AGB origin for these elements, together with near-normal abundances of magnesium, points to progenitor stars with initial masses in the range  $1.9 - 3 M_{\odot}$ .

There is not yet sufficient understanding of the chemical structure of CO white dwarfs, or of nucleosynthesis during a double white dwarf merger, to discriminate the origin (fossil or prompt) of all the abundance anomalies observed in EHe and RCB stars. Further work is required to quantify the expected yields of argon and s-process elements in the AGB intershell, and to improve the predicted yields of all elements from a *hot* merger.

**Key words:** stars: chemically peculiar (helium), stars: evolution, stars: abundances, stars: AGB and post-AGB, white dwarfs, binaries: close

## 1 INTRODUCTION

Extreme helium stars (EHe: spectral types O–A), R Coronae Borealis stars (RCB: spectral types F–G) and hydrogen-deficient carbon stars (HdC) are early- to late-type supergiants with atmospheres almost void of hydrogen, but highly enriched in carbon (Jeffery 2008; Clayton 1996;

\* E-mail: csj@arm.ac.uk

† E-mail: akarakas@mso.anu.edu.au

‡ E-mail: saio@astr.tohoku.ac.jp

Asplund et al. 2000). They display an extraordinary mixture of atomic species in ratios very different to those likely to have been established when the star was formed. In addition to hydrogen and helium, anomalies include large enrichments of nitrogen, oxygen, fluorine, neon and phosphorus, detections of lithium and s-process elements, overabundance in silicon and sulphur, together with a large range in iron abundance (Jeffery 1996; Rao & Lambert 1996; Pandey et al. 2006). It is commonly accepted that the hydrogen is a remnant of the outer layers of the original star, the enriched nitrogen comes from CNO-processed layers, helium from CNO-processed material and partially triple- $\alpha$ -processed material, and the carbon from  $3\alpha$  reactions (Heber 1983). There is increasing consensus concerning the origin of other elements, where the signature of material from the intershell (helium-rich) layers of asymptotic giant branch stars seems unmistakable (Pandey et al. 2006).

In order to interpret these abundances, it is necessary to infer some cataclysm in the history of the star by which the hydrogen-rich surface has been either ejected or consumed, whilst at the same time revealing a mixture of both CNO-processed helium,  $3\alpha$  processed helium, and other highly-processed material. This same process must also have involved the creation of a cool supergiant which is currently contracting to become a white dwarf (Schönberner 1986).

It was thought likely that EHe stars or RCB stars formed either following a final helium shell flash (or late thermal pulse) in a cooling white dwarf (Iben et al. 1983; Herwig 2000), or following a merger between a carbon-oxygen white dwarf and a helium white dwarf in a close binary (Webbink 1984; Saio & Jeffery 2002). Consensus now strongly favours the white dwarf merger origin, supported by evidence of evolution timescales, pulsation masses, and surface abundances (Saio & Jeffery 2002; Pandey et al. 2006; Clayton et al. 2007). Efforts are now focused on securing the abundance measurements and on the question of whether the merger is *cold* (no nucleosynthesis) or *hot*. For example, Clayton et al. (2007) argue that RCB overabundances of oxygen in general and  $^{18}\text{O}$  in particular are produced from nucleosynthesis during the merger, whilst Pandey & Lambert (2010) argue semi-quantitatively that no additional nucleosynthesis is required to match the observed abundances of H, He, C, N, O and Ne in EHe stars.

Evidently, we are far from an exhaustive understanding of (i) the evolution and (ii) the subsequent merger of two white dwarfs in a close binary. In the first instance, it is likely that the binary will have passed through at least one prior phase of common-envelope evolution. In the second, the merger of two white dwarfs involves the total destruction of the less massive star and the assimilation of a subsequent hot disk into the survivor. Both involve non-linear processes on dynamical timescales. Consequently, the accuracy with which current surface abundances may be used to infer past evolution may be legitimately challenged.

The object of this paper is to clarify the surface abundances which might arise under conservative assumptions for the merger of a helium white dwarf (HeWD) with a carbon-oxygen white dwarf (COWD) and to compare these with observed abundance anomalies. The question of predicted birthrates and galactic distribution of double-white dwarf mergers and their correlation with the observed distribution of EHe and RCB stars will be addressed in a separate paper.

**Table 2.** Notes to Table 1

A89	Anders & Grevesse (1989)
A00	Asplund et al. (2000)
C05	Clayton et al. (2005)
C06	Clayton et al. (2006)
C07	Clayton et al. (2007)
D98	Drilling et al. (1998)
J88	Jeffery (1988)
J92	Jeffery & Heber (1992)
J93a	Jeffery & Heber (1993)
J93b	Jeffery (1993)
J96	Jeffery et al. (1996)
J97	Jeffery & Harrison (1997)
J98	Jeffery (1998)
P01	Pandey et al. (2001)
P06a	Pandey et al. (2006)
P06b	Pandey (2006)
P06c	Pandey & Reddy (2006)
P08	Pandey et al. (2008)
P10	Pandey & Lambert (2010)

Thus, the known situation regarding surface abundances is reviewed in § 2. Background assumptions and calculations relating to the white dwarf merger model are discussed in § 3, particularly where these relate to the following. The mixing model used to infer merger surface abundances, together with the input from detailed stellar evolution and nucleosynthesis calculations, is described in § 4. The inferred elemental abundances are discussed in § 5. Finally, the sufficiency of the model is discussed in terms of whether additional nucleosynthesis is necessary. (§ 6).

## 2 THE OBSERVED SURFACE ABUNDANCES OF EHE AND RCB STARS

Over the last two decades, much effort has been expended on the accurate measurement of the surface abundances in EHe and RCB stars. These have been derived primarily from the analysis of high-resolution spectra using model atmospheres and theoretical line profiles which assume local thermodynamic, hydrostatic and radiative equilibrium (LTE). Model atmospheres have been computed using the codes MARCS (Asplund et al. 1997) for cool stars and STERNE (Jeffery et al. 2001) for hot stars. RCB and very cool EHe abundances are based on MARCS model atmospheres which use continuous opacities from the Opacity Project, and treat line opacities using opacity sampling. Published EHe abundances are based on STERNE models which use ATLAS6-type continuous opacities and an opacity-distribution function computed specifically for a hydrogen-poor carbon-rich mixture (Möller 1990).

It is important to note that although the abundances derived are in general consistent and not particularly sensitive to the model atmosphere structure, there are likely to be exceptions for individual elements. There are also improvements which could be made to the model atmospheres, and would lead to greater overall confidence in the derived abundances. For example, modern STERNE models include Opacity-Project continuous opacities and opacity-sampling for lines (Behara & Jeffery 2006). These have not yet been used in any detailed fine analysis of an EHe star,

Landscape table to go here:

**Table 1.** Observed abundances for EHe and RCB stars

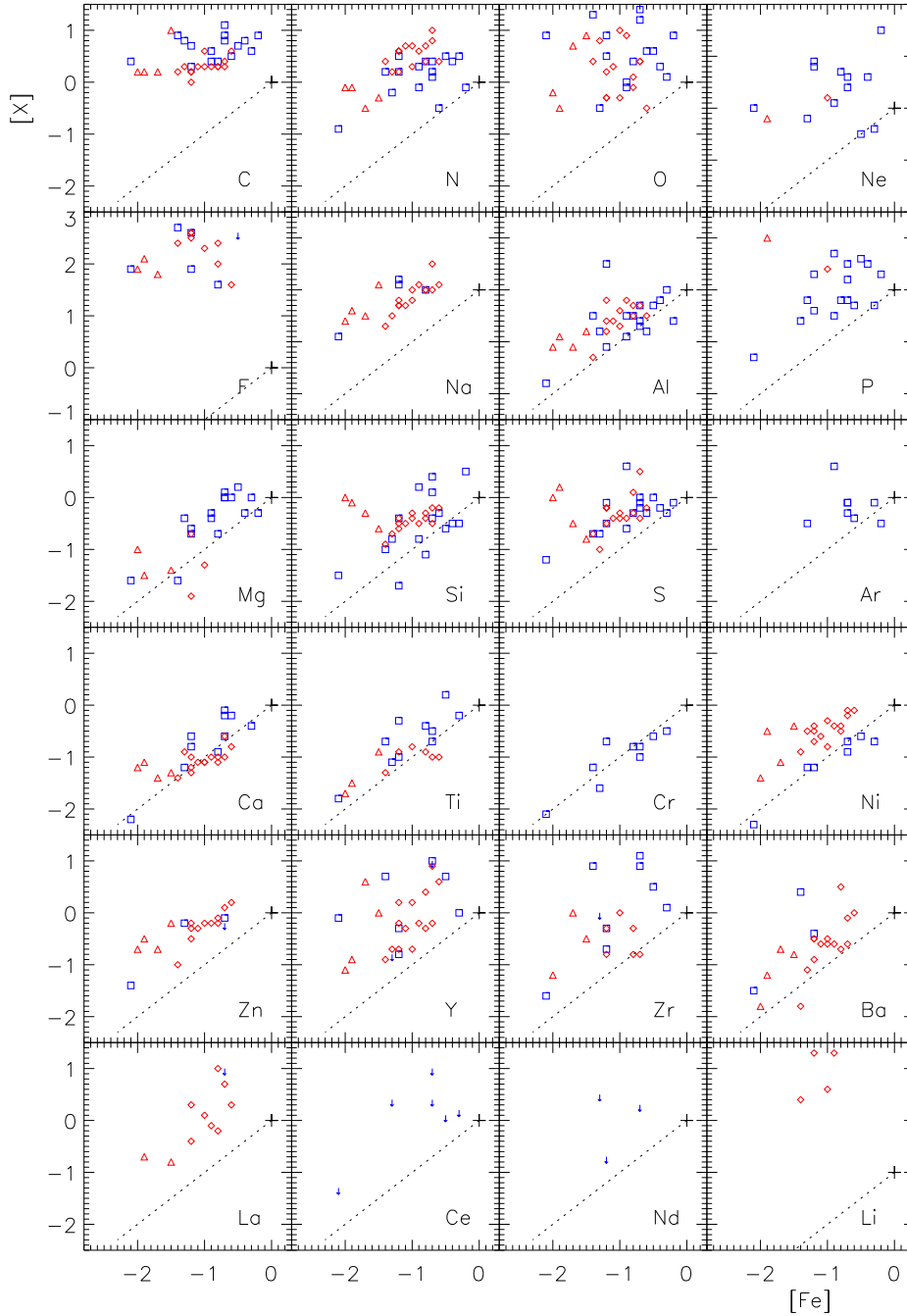


**Figure 1.** Observed surface abundances (log number relative to solar) versus iron abundance (same units) for extreme helium stars (blue squares), majority RCB stars (red diamonds), and minority RCB stars (red triangles). Upper limits are shown as arrows. The dotted line indicates a solar composition scaled to iron. Note that the plots for Ne, F, and Li are offset vertically; a cross indicates  $[Fe], [X] = 0, 0$  (solar abundance) in every case.

but do demonstrate sizable differences in temperature structure and overall flux distribution from the earlier models. For most RCB stars the major opacity source in the photosphere is carbon, but the most abundant species, helium, is not directly observable. This has led to a “carbon problem” whereby it is difficult to measure the carbon abundance unambiguously (Asplund et al. 1997; Pandey et al. 2004).

Since most EHe and RCB stars have low surface gravities, departures from LTE may also be important, particularly for the measurement of surface gravity and other quantities derived from strong lines (Jeffery 1998; Przybilla et al. 2005; Pandey & Lambert 2010).

For the present paper, published abundance data for EHe and RCB stars are collated and summarised in Tables 1

and 2. Abundances are cited in logarithmic units<sup>1</sup> such that

$$\epsilon_i \equiv \log n_i + C, \quad \sum n_i = 1, \quad (1)$$

where

$$\log \sum n_i \mu_i + C = \log \sum n_{i\odot} \mu_i + C_\odot \approx 12.15, \quad (2)$$

and the normalisations are such that the logarithmic hydrogen abundance of the Sun

$$\epsilon_{\text{He}\odot} \equiv 12.00. \quad (3)$$

Measurements have been rounded to 1 decimal place and given without errors; the reader should refer to the papers cited for more detail, but in general these are typically  $\pm 0.2 - 0.3$  dex. For space considerations, some elements measured in only a few stars have been omitted. Likewise, the HdC stars have been omitted, since iron abundances for these are not available. The EHe stars V652 Her (Jeffery et al. 1999) and HD 144941 (Harrison & Jeffery 1997; Jeffery & Harrison 1997) have been excluded for a different reason. They are comparatively hydrogen-rich, nitrogen-rich and carbon-poor, suggesting a different history. The measured iron abundance for DY Cen (5.0) is untypical of other elements (Jeffery & Heber 1993); unpublished data suggest a higher value. In this paper we assume an iron abundance for DY Cen scaled to that of aluminium, silicon and sulphur ( $\epsilon_{\text{Fe}} = 7.3$ ).

The emergence of overall patterns may be seen in Fig. 1 where each panel represents a different element, different symbols represent different groups of stars,  $[X] \equiv \epsilon_i - \epsilon_{i\odot}$  represents the (logarithmic) elemental abundance relative to the solar abundance, and  $[\text{Fe}]$  represents the iron abundance normalised in the same way. To understand this plot, consider that a star having the same composition as the Sun would appear at the origin (0,0) in every panel. Stars with elemental abundances scaling exactly with the iron abundance would lie on a straight line through the origin and having gradient unity (as indicated by a broken line). Similar plots have been presented and discussed in detail by Asplund et al. (2000) and Pandey et al. (2006). In summary, their conclusions were as follows.

## 2.1 Elements unaffected by evolution

*Iron:* several elements appear to be representative of initial metallicity. Fe may be adopted for spectroscopic convenience, and it is unlikely to be affected by H and He burning and attendant nuclear reactions. Pandey et al. (2006) find that Cr, Mn, and Ni vary in concert with Fe, so that these may also be taken as proxies for the initial metallicity.

$\alpha$ -elements: Mg, Si, S, and Ca and also Ti follow the expected trend in which the abundance ratio  $\alpha/\text{Fe}$  varies with Fe (Ryde & Lambert 2004; Goswami & Prantzos 2000) (with the possible exception of DY Cen: see above).

<sup>1</sup> Conventionally, stellar abundances are given logarithmically by number, normalised such the logarithmic hydrogen abundance is equal to 12. This convention assumes that hydrogen dominates the composition. In evolved mixtures, hydrogen may be vanishingly small, so the convention loses value. The formalism given here preserves abundance values ( $\epsilon_i$ ) of species unaffected, for example, by the conversion of hydrogen to helium.

*Aluminium:* abundances follow Fe with an apparent offset of about 0.4 dex.

*Argon:* in five out of seven EHes, Ar appears to have its initial abundance.

*Nickel:* although Ni varies in concert with Fe in both EHes and RCBs, there is a disconcerting offset of about 0.5 dex between the two groups. At this juncture, one suspects a systematic error due to the use of different ions or lines in the two groups of stars. The difference serves as a reminder that caution must be exercised with all abundance measurements discussed here.

*Zinc:* like Ni and Al, Zn correlates well with Fe, with a positive offset of  $\approx 0.8$  dex<sup>2</sup>. Again, one suspects a systematic error.

*Minority RCBs:* Lambert & Rao (1994) identify a subset of four RCBs which show lower Fe abundance and higher Si/Fe and S/Fe ratios than the majority. These are indicated in Table 1.

## 2.2 Elements affected by evolution

*Hydrogen:* excluding DY Cen and V854 Cen, the combined sample of EHes and RCBs have H abundances  $\log \epsilon_i$  in the range 4 - 8.

*Lithium:* a few RCBs are notably rich in lithium, which must have been produced simultaneously with or subsequent to the process which made these stars H-deficient (Asplund et al. 2000).

*Carbon:* excluding MV Sgr, the EHes show a mean carbon abundance  $\log \epsilon_i = 9.3$ , and a range from 8.9 - 9.7, corresponding to a mean C/He ratio of 0.006 and a range from 0.003 to 0.010. The carbon abundance is more difficult to measure reliably in RCBs; the mean indicated by Table 1 is apparently lower than in the EHes; this is probably a direct consequence of the carbon problem referred to above (Asplund et al. 1997).

In RCB and HdC stars cool enough to show CO, the  $^{12}\text{C}/^{13}\text{C}$  ratio is generally found to be greater than 100<sup>3</sup> (Warner 1967; Cottrell & Lambert 1982), confirming a 3- $\alpha$  or helium-burning origin for the carbon excess.

*Nitrogen:* nitrogen is enriched in the great majority of EHes and RCBs above that expected according to the Fe abundance (Fig. 1). Heber (1983) and subsequent authors point out that the N abundances in general follow the trend expected by the almost complete conversion of the initial C, N, and O to N via the H-burning CN and ON cycles. The exceptions are again DY Cen (very N-rich for its Fe abundance), and LSS 99 (very little N enrichment).

*Oxygen:* abundances relative to Fe range from underabundant by more than 1 dex to overabundant by almost 2 dex. The stars fall into two groups. Six EHes and a comparable number of RCBs with  $[\text{O}/\text{Fe}] \geq 1$  stand apart from the remainder which have an O abundance closer to their initial value. The O/N ratio for this remainder is approximately constant at  $\text{O}/\text{N} \approx 1$  and independent of Fe.

Both groups present problems. There is no obvious

<sup>2</sup> At very low metallicity, Zn is thought to be enhanced by the s-process, but not at levels which concern us here.

<sup>3</sup> the exception being V CrA with  $^{12}\text{C}/^{13}\text{C} \approx 4$  (Rao & Lambert 2008)

means to produce  $[O/Fe] \geq 1$  (in most of these cases it is impossible to distinguish  $^{16}O$  from  $^{18}O$ ). For the remainder, nearly all have an N abundance indicating total conversion of initial C, N, and O to N via the CNO cycles, so that an observed O abundance so close to the initial abundance is unexpected. It could be partially accounted for by dredge-up of  $^{16}O$  from the CO-core during post-AGB evolution, as has been suggested to explain high O abundances in PG1159 stars (Werner & Herwig 2006).

Another solution is suggested by the remarkable discovery that the  $^{18}O/^{16}O$  ratio in RCB stars (where observed) is close to and sometimes greater than unity, a ratio many hundreds of times higher than expected (Clayton et al. 2005, 2007). In HdC stars, the  $^{18}O/^{16}O$  ratios are even higher (García-Hernández et al. 2009, 2010). However, there is as yet insufficient evidence to indicate that the excess O is in the form of  $^{18}O$  in *all* RCBs or in any EHes.

Knowing that early-asymptotic giant branch stars possess a high  $^{18}O/^{16}O$  pocket in a thin layer of the He-burning shell, Warner (1967) speculated that under unusual circumstances a star might strip all of its envelope material precisely down to this narrow layer, but Clayton et al. (2005) concludes this to be highly improbable.

*Fluorine*: the discovery of very substantial quantities of fluorine, first in several EHes and subsequently in most RCBs, was also unexpected (Pandey 2006; Pandey et al. 2008). It appears to be uncorrelated with Fe or O and is overabundant by 2 – 4 dex. F is produced in the He-intershell of an AGB star through a (complex) combination of  $\alpha$ -, n- and p-capture reactions (Lugaro et al. 2004), a conclusion confirmed by an observed correlation between C and F in the atmospheres of AGB stars (Jorissen et al. 1992; Abia et al. 2010), and by observations of post-AGB stars that show F at the level predicted to be in the intershell (Werner et al. 2009).

*Neon*: high overabundances derived from NeI lines for a few intermediate temperature EHes were originally treated with scepticism – non-LTE being a possible culprit. A similar overabundance measured from NeII lines in LSIV+6°2 (Jeffery 1998) effectively substantiated the NeI results in other stars. Pandey & Lambert (2010) have made a recent non-LTE analysis of the neon abundances in three EHes, and confirmed a substantial overabundance approximately independent of the star’s iron abundance.  $^{22}Ne$  is produced via two  $\alpha$ -captures on  $^{14}N$ , so should be abundant in carbon-rich material derived from helium produced by the CNO-process.

*Phosphorus*: an overabundance of P was first remarked in BD+10°2179 by Hunger & Klinglesmith (1969). This was discounted from ultraviolet spectroscopy by Heber (1983) and Pandey et al. (2006). Overabundances have been reported in several other EHes by *inter alia* Kaufmann & Schönberner (1977); Jeffery & Heber (1992, 1993); Jeffery (1993), where they are systematically larger than in the sample studied by Pandey et al. (2006). Whether this represents a problem with *gf*-values deserves further investigation. P can be produced through neutron captures in an asymptotic giant branch star (of which more later). As the observations stand, P overabundances may be a key diagnostic of previous history.

*Heavy elements*: two EHes are severely enriched in Y and Zr: V1920 Cyg and LSE 78 with overabundances of about a factor of 50 (Pandey et al. 2004). A third, PV Tel, is enriched

**Table 3.** Galactic merger rates for double white dwarf binaries.

Source	He+He	He+CO : CO+He yr <sup>-1</sup>	CO+CO
Webbink (1984) <sup>1</sup>	2.9	1.9 $\times 10^{-11} \text{pc}^{-2} \text{yr}^{-1}$	1.2
Iben et al. (1996)		0.0023	
Han (1998) <sup>2</sup>	0.0112	0.0154	0.0044
Nelemans et al. (2001)		0.0044	
Yu & Jeffery (2010)		0.0027	

<sup>1</sup> It is not clear whether Webbink reports the double-degenerate birth rate or merger rate.

<sup>2</sup> Model Set 1: merger rate = birth rate assumes all DD’s will merge

by a factor of about 10. Five other stars for which measurements were possible are considered to have their initial abundances of Y and Zr. Y and Zr overabundances are attributed to contamination by s-process products. The origin of these has not been identified.

Only upper limits are reported for rare earth elements La, Ce, and Nd, all consistent with the observed abundances of Zr and Y. The cool EHe LSIV–14°109 has a Ba abundance consistent with its initial metallicity.

### 2.3 Key Questions

The surfaces of RCBs and EHes primarily exhibit CNO-processed helium. In addition, they show contamination by a residue of hydrogen, by  $3\alpha$ -processed carbon, and by additional  $\alpha$ -capture products.

The primary challenge is to demonstrate a mechanism which will deliver the observed mixture, or range of mixtures, at the stellar surface. This mechanism must also be able to explain large overabundances of Li,  $^{18}O$ ,  $^{19}F$ , possibly P, and various s-process elements.

## 3 MODELS FOR THE EVOLUTION OF CO+HE WD MERGERS

While evidence has accrued in favour of an origin involving the merger of a carbon-oxygen white dwarf with a helium white dwarf, this has not always been the favoured model. Valid questions include whether such mergers can occur, with what frequency, and with what outcomes.

### 3.1 The formation of CO+He binary white dwarfs

Webbink (1984) first recognised that one consequence of close binary evolution would be the formation and evolution of double white-dwarf binary (DWD) systems that could ultimately merge.

The evolution of a main-sequence star results in an expansion that will bring it into contact with a sufficiently nearby companion. Such contact may result in stable Roche lobe overflow, or dynamical mass transfer, resulting in the formation and ejection of a common envelope. The outcomes depend on the binary mass ratio and on the structure of the larger star, and are diverse (Iben & Tutukov 1985). The remnants include double helium white dwarfs;

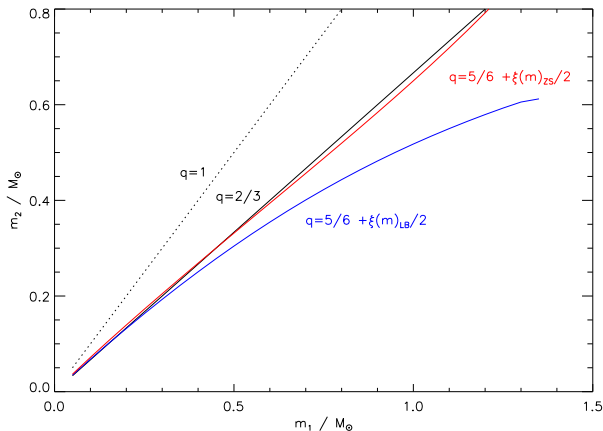


**Figure 2.** Stability limits for mass transfer in close double white dwarfs. Above the appropriate limit, mass transfer should be dynamically unstable. The limits  $\xi_{\text{LB}}$  and  $\xi_{\text{ZS}}$  refer to cold WD mass-radius relations due to Lynden-Bell & Tout (2001) and Nelemans et al. (2001) respectively.

carbon-oxygen plus helium white dwarfs, and double carbon-oxygen white dwarfs. Webbink (1984) estimated birth rates for the formation of each of these systems; similar estimates have formed one output of many subsequent binary-star population-synthesis studies of the Galaxy.

Up to the mid 1980’s, a criticism of theory was the absence of hard observational evidence that short-period white-dwarf binaries actually do form, whether as a consequence of close-binary evolution or otherwise. This problem was largely addressed by the discovery of significant numbers of such systems (Saffer et al. 1988; Marsh 1995; Marsh et al. 1995). Further discoveries were made as a result of large-scale white dwarf surveys (Napiwotzki et al. 2003; Nelemans et al. 2005; Morales-Rueda et al. 2005).

At present, there exists a qualitative agreement between observed DWD space densities and their predicted birth rates. The question, as it applies to DWD mergers, will be addressed in more detail elsewhere (Jeffery et al. in preparation).

### 3.2 Gravitational-wave radiation and dynamical mergers

There are two principles behind the idea that close-binary white dwarfs will merge to form a single star.

The first principle is that angular momentum is removed from the binary by means of gravitational radiation (GR) and that, within a Hubble timescale, the less massive and consequently larger white dwarf will eventually fill its Roche lobe and a phase of mass transfer will begin. The timescale for orbital decay by GR is given by

$$(\tau/y) = 10^7 (P/h)^{8/3} \mu^{-1} (M/M_{\odot})^{-2/3}, \quad (4)$$

where  $P$  is the orbital period,  $M = m_1 + m_2$  is the total mass of the system and  $\mu$  is the reduced mass (Landau & Lifshitz 1958; Marsh et al. 1995), indicating that DWD systems with  $P \lesssim$  a few hours will reach contact within a Hubble time.

The second principle is that if the mass ratio

$$q \equiv m_2/m_1 \geq q_{\text{crit}} \equiv \frac{5}{6} + \frac{\xi(m_2)}{2}, \quad (5)$$

the increase of radius due to the reduction of mass ( $\xi(m) \equiv d \ln r / d \ln m$ ) will exceed the increase in the Roche radius caused by the transfer of angular momentum. Mass transfer then becomes dynamically unstable and probably causes the components to coalesce (Pringle & Webbink 1975; Tutukov & Yungelson 1979). For this paper we have adopted the mass-radius relation for a cold white dwarf reported by Lynden-Bell & Tout (2001), with  $\beta = 1.137$  and  $\mu_e = 2.02$ . Note that this relation, which is valid from sub-planetary masses through to relativistic white dwarfs, gives  $\xi(m)$  markedly different to that used by Nelemans et al. (2001), which lies very close to the classical non-relativistic  $r \propto m^{-1/3}$  relation (Fig. 2).

For smaller  $q$ , mass transfer will be stable; but if the mass-transfer rate exceeds the Eddington rate, the envelope of the accretor will heat and expand leading to the possible formation of a common envelope and which could also cause the stars to coalesce (Han & Webbink 1999). Only at the most extreme mass ratios will mass transfer be stable, possibly leading to the formation of AM CVn systems (He+He WDBs) (Nather et al. 1981). Significantly, *all* of the DWD systems for which mass ratios could be measured (Maxted et al. 2002) have  $q > q_{\text{crit}}$ .

Using this information together with DWD birth rates, population synthesis studies indicate a DWD merger frequency for the Galaxy of between  $2.3 - 4.4 \cdot 10^{-3} \text{y}^{-1}$  (Iben 1990; Nelemans et al. 2001; Yu & Jeffery 2010). Other estimates are indicated in Table 3, broken down by binary type wherever possible.

Of particular interest, of course, is the frequency of double COWD mergers, since these are a possible (Webbink 1984; Iben & Tutukov 1984) but arguable (Saio & Nomoto 2004; Yoon & Langer 2005) source of Type Ia supernovae (SN Ia). Other outcomes are more likely (Iben & Tutukov 1984; Saio & Nomoto 1995, 1998). Double HeWD mergers may produce sdO (Webbink 1984) or sdB (Iben 1990) stars, which are ubiquitous in old stellar populations (Brown et al. 2001; Busso et al. 2005; Lee et al. 2005; Rich et al. 2005).

### 3.3 SPH simulations of the dynamical merger

Several simulations of the white dwarf merger process have been attempted using smoothed particle hydrodynamics (Benz et al. 1990; Segretain et al. 1997; Guerrero et al. 2004; Yoon et al. 2007; Lorén-Aguilar et al. 2009). For CO+He WD mergers (*e.g.*  $0.6+0.4 M_{\odot}$ ), these demonstrate the total disruption of the low-mass WD within roughly one orbital revolution ( $\sim 90\text{s}$ ) and the conservation of  $\sim 99\%$  of its mass within a thick Keplerian disk. They also demonstrate substantial prompt heating of the disrupted material, with temperatures momentarily reaching several  $10^9 \text{K}$  in the equatorial plane (Guerrero et al. 2004). However, the temperatures are not extremely high, the degeneracy of the disrupted material is rapidly lifted, and any thermonuclear activity is ultimately quenched.

### 3.4 Nucleosynthesis during a dynamical merger

In previous discussion of the post-merger product, Saio & Jeffery (2002) made the simplifying assumption that *no* nucleosynthesis occurs during the merger – this is the *cold* merger approximation.

Where  $^{12}\text{C}$  and  $^4\text{He}$  mix at sufficiently high temperatures, some thermonuclear activity will occur. Any  $^{14}\text{N}$  will also be briefly exposed to  $\alpha$ -burning. Using an elegant one-zone model in which orbital energy is converted to heat in a debris disk, Clayton et al. (2007) showed that certain nuclear abundances could be demonstrably altered during the merger. In particular, surplus  $^{18}\text{O}$  could be produced through prompt nucleosynthesis of  $^{14}\text{N}$  and  $^4\text{He}$  from the debris of the helium white dwarf<sup>4</sup>, without being subsequently destroyed by an additional  $\alpha$ -capture to form  $^{22}\text{Ne}$ .

Lorén-Aguilar et al. (2009) included a limited nuclear network in their dynamical merger simulation, and reported nuclear yields for various DWD progenitor combinations. Models which include some nucleosynthesis during white dwarf destruction will be referred to as the *hot merger* approximation.

Since the physics of DWD mergers is of substantial wider interest for the production of hot subdwarfs and SN Ia, the question of whether mergers are *hot* or *cold* is particularly relevant. Rephrasing: to what extent does nucleosynthesis occur as a direct consequence of heat generated by orbital energy dissipated during the merger, and do any nuclear products play a rôle in the subsequent evolution? In particular, is a *hot merger* necessary to explain the high  $^{18}\text{O}/^{16}\text{O}$  ratio observed in RCB stars?

### 3.5 Models of thermal and nuclear evolution after a merger

The evolution of a WD rapidly accreting helium was first considered long before the possibility of DWD mergers was widely recognised (Nomoto & Sugimoto 1977). This and subsequent calculations pursued the evolution of the accretor through and beyond off-centre helium ignition (Nomoto & Hashimoto 1987; Kawai et al. 1987, 1988; Iben 1990; Saio & Nomoto 1998; Saio & Jeffery 2000, 2002).

Such models have been used to approximate evolution following a dynamical merger by making some working assumptions. These include the less massive white dwarf being completely disrupted by the merger, forming a Keplerian disk and subsequently being assimilated onto the surface of the accretor. Assimilation has been assumed to be by spherical accretion at half the Eddington rate<sup>5</sup> ( $\approx 10^{-5}M_{\odot}\text{y}^{-1}$ ). Accretion was switched off once a pre-selected final mass was attained.

Conceptually, this approach is flawed. It implies that, following shell-helium ignition and subsequent expansion, the reservoir of material to be accreted (*i.e.*, the remnant of the disrupted white dwarf) remains in a Keplerian disk deeply embedded within the giant envelope. Although

such a disk might survive, it runs counter to the principle that viscous disks collapse on a much shorter timescale (Lynden-Bell & Pringle 1974). The disk is more likely to heat and expand to form a high-entropy envelope in hydrostatic equilibrium (Yoon et al. 2007).

In their simulations Saio & Jeffery (2002) assumed all accreted material to be deposited on the surface of the accretor, and to have a composition defined by the mean composition of a helium white dwarf. The chemical structure of the accreting CO white dwarf was obtained by evolving a star from the zero-age main sequence through to an appropriate point on the white-dwarf cooling sequence.

During post-merger evolution, there are two phases of convective mixing. The first is bottom-up nuclear-driven convection immediately following shell-helium ignition. In the Saio & Jeffery (2000, 2002) models, this occurs when the envelope mass is small, and does not produce very much mixing. Subsequent top-down opacity-driven convection develops when the star becomes a giant, and does not reach layers enriched by post-merger nucleosynthesis. The models consequently show very little chemical enrichment at the surface from C, O or other nuclear products due to this mixing.

The relative absence of  $^{12}\text{C}$  or  $^{16}\text{O}$  in the Saio & Jeffery (2002) COWD intershell contradicts the substantial enhancements predicted in the AGB intershell (*e.g.* Herwig (2000)), possibly because chemical evolution through the thermal-pulsing AGB was not treated in sufficient detail. Some additional merger sequences were therefore computed with enhanced  $\beta_{12\text{C}} = 0.2$  and  $\beta_{16\text{O}} = 0.05$ , where  $\beta_i$  represents the mass fraction of species *i*.

Consequently, Saio & Jeffery (2002) argued that the dynamical merger would have to disrupt the outer layers of the COWD in order to explain the observed EHe and RCB surface abundances of C. Scrutiny shows that the *simple recipe* adopted by Saio & Jeffery (2002), and also by Pandey et al. (2001, 2006); Pandey & Lambert (2010), requires further refinement.

First, the COWD models would benefit from a more realistic abundance distribution, particularly in the helium layer, which should have the composition of the intershell region of the progenitor AGB star.

Second, it was not appreciated that some COWD models (*e.g.* Saio & Jeffery 2002) might contain a substantial pocket of  $^{18}\text{O}$  at the interface between the CO-core and the He intershell, as well as a reservoir of  $^{22}\text{Ne}$  in the CO-core. Thus, if the outer layers of the CO-core are disrupted during the merger, substantial  $^{18}\text{O}$  and  $^{22}\text{Ne}$  will be dredged up in addition to  $^{12}\text{C}$ .

This question is somewhat open. Not all post-AGB models show this  $^{18}\text{O}$  pocket. Depending on the intershell temperatures,  $^{14}\text{N}$  may be completely destroyed by  $\alpha$ -capture to  $^{22}\text{Ne}$  *before* the helium-burning shell passes it into the CO core.

The object of the following sections is therefore to refine the *simple recipe* used in previous discussions of EHe and RCB surface abundances, to incorporate a more realistic description of the chemistries involved, and hence to develop a more quantitative framework in which to discuss white dwarf mergers as possible progenitors.

<sup>4</sup> The reactions involved are:  $^{14}\text{N}(\alpha, \gamma)^{18}\text{F}(\beta^+)^{18}\text{O}$

<sup>5</sup> This rate was chosen to avoid a runaway explosion (for low accretion rates) and to satisfy energy conservation. Higher accretion rates would be possible if heat could be removed apherically.

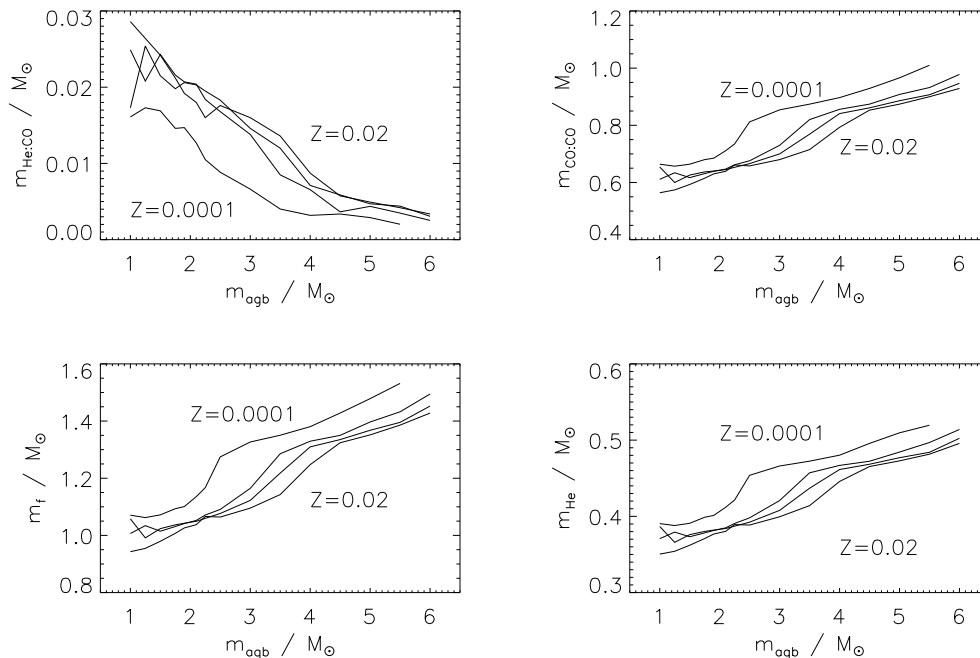


**Figure 3.** Masses of the merger components as a function of the initial mass of the COWD progenitor ( $m_{\text{agb}}$ ) and of the initial system metallicity ( $Z = 0.0001, 0.004, 0.008$  and  $0.02$ ).  $m_{\text{He:CO}}$  represents the final mass of the AGB intershell before the star contracts to become a COWD.  $m_{\text{CO:CO}}$  represents the mass of the carbon-oxygen core at the same time.  $m_{\text{He}}$  represents the mass of the HeWD secondary given by Eq. 12.  $m_f$  represents the total mass of the product, assuming a conservative merger.

## 4 THE SIMPLE RECIPE

### 4.1 Masses

As is evident from the preceding summary, the processes by which two white dwarfs may merge are far from straightforward. In addition, the overall distribution of elements in both stars is a function of the initial masses, metallicity and period in the original binary system. To become a COWD, the ultimately more massive star must first ascend the asymptotic giant branch, during which time the helium-rich intershell will be processed by a series of thermal pulses, whilst the hydrogen-rich envelope will be enriched by multiple convective dredge-up episodes. To create a close binary which will ultimately merge, the system must pass through one or more common-envelope phases, producing an abrupt change in the mass (at least) of one or both components. During the merger, the less massive white dwarf will be completely disrupted to form (a) a Keplerian disk and (b) a hot corona (Yoon et al. 2007; Lorén-Aguilar et al. 2009). During the disruption episode, temperatures and densities may become high enough for nucleosynthesis. Shear mixing between the disk, corona and the surface of the more massive white dwarf seems inevitable, though how deep such mixing would be remains to be explored. Subsequently, material from the disk and corona will be accreted onto the surface of the more massive white dwarf; the assumption is that it will be chemically homogenised. As this hot material forces the star to expand and cool, surface convection zones will develop from the surface. Flash-driven convection will develop following helium-shell ignition. Most of these processes are poorly understood. Where numerical

models do exist, *e.g.* for the dynamical phases (Yoon et al. 2007; Lorén-Aguilar et al. 2009), or for the nuclear phases (Saio & Jeffery 2002), they are not yet joined up.

Until such time as they are, some simplifying assertions allow us to make order-of-magnitude arguments. The principal of these is that all material from the helium white dwarf, and all hydrogen-rich and helium-rich material from the carbon-oxygen white dwarf will be fully mixed during the dynamical phase of the merger. From the point of view of developing a recipe for calculating the chemical signature of the merged product, this assertion gives us the first set of parameters that will be required, namely the masses associated with each layer of material to be mixed. We adopt the notation  $m_{j:k}$  to represent the mass of layer  $j$  of star  $k$  (see also Saio & Jeffery 2002), thus:

- $m_{\text{H:He}}$ : the mass of the hydrogen-rich surface layer of the HeWD;
- $m_{\text{He:He}}$ : the mass of the helium core of the HeWD;
- $m_{\text{H:CO}}$ : the mass of the hydrogen-rich surface layer of the COWD; and
- $m_{\text{He:CO}}$ : the mass of the helium shell of the COWD.

This principal assertion actually takes two forms. In the conservative case, all material from both white dwarfs is included in the merged product. In the non-conservative case, some mass may be lost under which circumstance the above parameters represent the layer masses which survive the merger. SPH calculations suggest that white-dwarf mergers are conservative (Guerrero et al. 2004; Lorén-Aguilar et al. 2009).

Without additional processing, none of these layers con-

tains sufficient carbon to account for the abundances observed in EHe, RCB and HdC stars. As in previous applications of this recipe, it is necessary to make a second assertion that some material from the outer edge of the carbon-oxygen core of the COWD has been somehow included into the mixture. For now, we define:

$m_{\text{CO:CO}}$ : the mass of the carbon-oxygen core of the COWD; and

In addition, we have the total masses:

$m_{\text{He}}$ : the total mass of the HeWD;  
 $m_{\text{CO}}$ : the total mass of the COWD;  
 $m_{\text{f}}$ : the final mass of the merged product.

In the conservative case, the number of variables is reduced since:

$$m_{\text{f}} = m_{\text{He}} + m_{\text{CO}}, \quad (6)$$

$$m_k = \sum_j m_{j:k}; \quad j = \text{H, He, CO}, k = \text{He, CO}. \quad (7)$$

Also, since helium (in general) dominates the final mixture and

$$m_{\text{He:He}} \gg m_{\text{He:CO}} \gg m_{\text{H:CO}} \approx m_{\text{H:He}}, \quad (8)$$

the observed hydrogen abundance naturally constrains the masses of the hydrogen-rich layers:

$$\beta_{\text{H}}/\beta_{\text{He}} \approx (m_{\text{H:CO}} + m_{\text{H:He}})/m_{\text{He:He}}, \quad (9)$$

where  $\beta_i$  represents the abundance by mass fraction of species  $i$  ( $\sum_i \beta_i \equiv 1$ ). Since in general EHes and RCBs show  $\epsilon_{\text{H}}/\epsilon_{\text{He}} \approx \beta_{\text{H}}/(\beta_{\text{He}}/4) < 10^{-4}$ , we conclude

$$m_{\text{H:CO}} + m_{\text{H:He}} < 10^{-4} m_{\text{He:He}}. \quad (10)$$

We have attempted to use a similar argument to estimate the mass of the carbon-oxygen core to be included in the mixed layers ( $m_{\text{mix:CO}}$ ) by supposing that the observed C and O come entirely from the COWD core;

$$(\beta_{\text{C}} + \beta_{\text{O}})/\beta_{\text{He}} \approx m_{\text{mix:CO}}/m_{\text{He:He}}. \quad (11)$$

It will be seen that this approach is too crude.

With five masses to be adjusted in order to account for the abundances of hydrogen, helium, carbon, nitrogen and oxygen, the recipe appears under-constrained. Fortunately, stellar evolution theory provides additional information.

For example, Saio & Jeffery (2002) noted that in the conservative case for a  $0.6 M_{\odot}$  carbon-oxygen white dwarf merging to form a  $0.9 M_{\odot}$  product, the donor would likely have been predominantly helium with a mass  $m_{\text{He:He}} = 0.3 M_{\odot}$ . On its surface would have been a hydrogen-rich envelope of mass  $m_{\text{He:H}} \approx 10^{-3} - 10^{-4} M_{\odot}$  (Driebe et al. 1998), reduced to this value by Roche lobe overflow during its first ascent of the giant branch.

We now introduce the notion that a similar connection exists between the carbon-oxygen white dwarf and the initial star in the binary system. Assuming that both stars evolve as single stars up to the point of merger<sup>6</sup>, then models of

stellar evolution through to the late asymptotic giant branch (Karakas 2010) (Fig. 3) give values for  $m_{\text{He:CO}}$  and  $m_{\text{CO:CO}}$  in terms of

$m_{\text{agb}}$ : the initial mass of the star which becomes a COWD.

Such models also give a value for the mass of the AGB star hydrogen envelope, but most of this will be substantially removed by stellar winds and may form a planetary nebula before the star becomes a white dwarf.

Establishing the mass of the COWD as a function of its progenitor mass, the mass of the HeWD must lie below the minimum mass for core helium ignition, approximately  $0.48 M_{\odot}$ , and above the critical value for stable mass transfer (§ 3.2). To restrict the number of free parameters in our model, we therefore set

$$m_{\text{He}} = q_{\text{crit}} m_{\text{CO}}, \quad (12)$$

the lower limit for dynamical mergers (Eq. 5). This automatically prescribes the ratio  $m_{\text{He:He}} : m_{\text{He:CO}}$  for a given  $m_{\text{CO}}$  and  $Z$ , and hence determines the dilution by the helium white dwarf of elements produced in the AGB inter-shell. However, we note that more massive HeWDs may exist, and that less massive HeWDs may merge as a result of a common-envelope phase.

Thus, our *simple recipe* for predicting the surface abundances of the product of a *cold, conservative* He+COWD merger now only requires  $m_{\text{i:CO}}$  and  $Z$  as primary inputs, together with a prescription for the composition of each component of the mixture.

## 4.2 Composition

We introduce the notation  $\beta_{ijk}$  to refer to the mass fraction of species  $i$  in layer  $j$  of component  $k$ . Generally  $i \equiv z$ , the atomic number. We currently consider the abundances of:  $^1\text{H}$ ,  $^4\text{He}$ ,  $^{12}\text{C}$ ,  $^{13}\text{C}$ ,  $^{14}\text{N}$ ,  $^{16}\text{O}$ ,  $^{18}\text{O}$ ,  $^{19}\text{F}$ ,  $^{22}\text{Ne}$ ,  $^{23}\text{Na}$ ,  $^{24}\text{Mg}$ ,  $^{27}\text{Al}$ ,  $^{28}\text{Si}$ ,  $^{31}\text{P}$ ,  $^{32}\text{S}$ ,  $^{40}\text{Ar}$ ,  $^{40}\text{Ca}$ ,  $^{48}\text{Ti}$ ,  $^{51}\text{V}$ ,  $^{52}\text{Cr}$ ,  $^{55}\text{Mn}$ ,  $^{56}\text{Fe}$ ,  $^{59}\text{Co}$ , and  $^{59}\text{Ni}$ .

Assuming the binary system was established with an initial metallicity  $Z$ , the composition of the hydrogen-rich layers in both components is then defined by a scaled solar composition ( $\beta_{i\odot}$ ). We adopt:

$$\beta_{i:\text{H:He}} = \alpha_i(Z) \beta_{i\odot} \cdot Z/Z_{\odot}, \quad i > 2, \quad (13)$$

$$\beta_{\text{He:H:He}} = 0.28, \quad (14)$$

$$\beta_{\text{H:H:He}} = 1 - \sum_{i>1} \beta_{i:\text{H:He}}, \quad (15)$$

$$\beta_{i:\text{H:CO}} = \beta_{i:\text{H:He}}. \quad (16)$$

Generally,  $\alpha_i = 1$ , but in metal-poor environments ( $Z < Z_{\odot}/10$ ) the abundances of  $^{16}\text{O}$ ,  $^{18}\text{O}$ , Mg, Si, S, Ca, Ti and Mn are observed to exceed the scaled solar value by as much as 0.5 dex (Goswami & Prantzos 2000; Ryde & Lambert 2004).  $\alpha_i(Z)$  has been chosen accordingly. The last relation implies that dredge-up into the H-envelope has been ignored, especially dredge-up on the AGB, but also dredge-up prior to the AGB. This is justified because  $m_{\text{H:CO}}$  is so small that, apart from hydrogen, this layer makes a negligible contribution to the merger composition.

<sup>6</sup> The fully self-consistent approach would be to find the initial binary ( $m_1, m_2, P_{\text{orb}}$ ) that will produce a close white dwarf pair of appropriate dimensions and then to compute the evolution of both components in detail, including their passage through any mass transfer or common-envelope phases.

#### 4.2.1 HeWD core

The composition of the HeWD core is assumed to have been produced by CNO-cycle hydrogen burning. This converts practically all of the carbon and oxygen (depending on temperature) to  $^{14}\text{N}$ . To allow for incomplete CNO cycling in low-mass stars, we introduce the branching ratio  $f_{\text{CNO}}$  between the full CNO cycle and the CN cycle. The composition is then given by:

$$\beta_{i:\text{He:He}} = \beta_{i:\text{H:He}}, \text{ except } \dots \quad (17)$$

$$\beta_{^{12}\text{C}:\text{He:He}} = 0, \quad (18)$$

$$\beta_{^{13}\text{C}:\text{He:He}} = 0, \quad (19)$$

$$\beta_{^{14}\text{N}:\text{He:He}} = \Sigma_{\text{C,N}}\beta_{i:\text{H:He}} + f_{\text{CNO}}\Sigma_{\text{O}}\beta_{i:\text{H:He}}, \quad (20)$$

$$\beta_{^{16}\text{O}:\text{He:He}} = (1 - f_{\text{CNO}})\beta_{^{16}\text{O}:\text{H:He}}, \quad (21)$$

$$\beta_{^{18}\text{O}:\text{He:He}} = (1 - f_{\text{CNO}})\beta_{^{18}\text{O}:\text{H:He}}, \quad (22)$$

$$\beta_{\text{H}:\text{He:He}} = 0, \quad (23)$$

$$\beta_{\text{He:He:He}} = 1 - \Sigma_{i \neq 2}\beta_{i:\text{He:He}}. \quad (24)$$

$\Sigma_i$  represents a sum over all isotopes of species  $i$ . So far, we have always used  $f_{\text{CNO}} = 1$ , implying the full CNO cycle.

#### 4.2.2 COWD shell

The helium-rich layer of the COWD corresponds to the intershell of the progenitor AGB star. The composition of this layer is the most interesting of all since it contains a combination of CNO-cycled helium, various  $\alpha$ -capture products, and the products of a nuclear network which includes s-process neutron-capture products. The yield of each isotope from these processes is a sensitive function of the initial abundances and of the temperatures and densities throughout successive thermal-pulse cycles of the AGB star. Given the importance of this layer to the final composition of the merged product, we have adopted intershell compositions from a grid of full AGB-star evolution calculations (Karakas 2010). These provide fractional abundances for  $^4\text{He}$ ,  $^{12}\text{C}$ ,  $^{16}\text{O}$ ,  $^{17}\text{O}$ ,  $^{18}\text{O}$ ,  $^{19}\text{F}$ ,  $^{20}\text{Ne}$ ,  $^{21}\text{Ne}$ ,  $^{22}\text{Ne}$ ,  $^{23}\text{Na}$ ,  $^{24}\text{Mg}$ ,  $^{25}\text{Mg}$ ,  $^{26}\text{Mg}$ ,  $^{27}\text{Al}$ ,  $^{28}\text{Si}$ ,  $^{29}\text{Si}$ ,  $^{30}\text{Si}$ ,  $^{31}\text{P}$ ,  $^{32}\text{S}$ ,  $^{33}\text{S}$ , and  $^{34}\text{S}$  and define  $\beta_{i:\text{He:CO}}$  for these species. In our recipe, the isotopes of Ne, Mg, Si and S, are combined, since these are not resolved observationally.  $^{13}\text{C}$  and  $^{14}\text{N}$  are destroyed in the intershell, with  $^{14}\text{N}$  being converted to  $^{22}\text{Ne}$ . Thus:

$$\beta_{\text{H}:\text{He:CO}} = 0, \quad (25)$$

$$\beta_{^{13}\text{C}:\text{He:CO}} = 0, \quad (26)$$

$$\beta_{^{14}\text{N}:\text{He:CO}} = 0. \quad (27)$$

The AGB model grid of Karakas (2010) provides information about light-element abundances, core and shell masses in post-AGB stars over a large range of  $m_{\text{agb}}$  and  $Z$ , but lacks detailed information for s-process elements. Consistent calculations for Zn, Y, Zr, Ba, La, Ce and Nd are available for one model with  $m_{\text{agb}} = 2 M_{\odot}$ ,  $Z = 0.0001$  (Lugaro et al. 2011, in preparation) and one with  $m_{\text{agb}} = 3 M_{\odot}$ ,  $Z = 0.02$ . We have used these as indicative of the range of s-process yields in AGB stars of intermediate initial mass.

#### 4.2.3 COWD core boundary

The outer layers of the carbon-oxygen core of the COWD will obviously lack hydrogen and helium and be dominated by  $^{12}\text{C}$  and  $^{16}\text{O}$  from the  $3\text{-}\alpha$  and  $^{12}\text{C}(\alpha, \gamma)^{16}\text{O}$  reactions.

An initial approach was to adopt a factor  $f_{\text{CO}} \equiv \beta_{^{12}\text{C}}/(\beta_{^{12}\text{C}} + \beta_{^{16}\text{O}}) = 0.8$  based on typical abundances for COWD cores from contemporary computations. Since the outer layers of the core will be those which most recently exited the base of the intershell, the abundances of most other elements can be set equal to those of the intershell:

$$\beta_{\text{H}:\text{CO:CO}} = 0, \quad (28)$$

$$\beta_{\text{He}:\text{CO:CO}} = 0, \quad (29)$$

$$\beta_{^{16}\text{O}:\text{CO:CO}} = (1 - f_{\text{CO}})(\beta_{\text{He:He:CO}} + \beta_{^{12}\text{C}:\text{He:CO}} + \beta_{^{16}\text{O}:\text{He:CO}}) \quad (30)$$

$$\beta_{^{12}\text{C}:\text{CO:CO}} = f_{\text{CO}}(\beta_{\text{He:He:CO}} + \beta_{^{12}\text{C}:\text{He:CO}} + \beta_{^{16}\text{O}:\text{He:CO}}) \quad (31)$$

$$\beta_{i:\text{CO:CO}} = \beta_{i:\text{He:CO}}, \quad i \neq 1, 2, 6, 8 \quad (32)$$

Apart from the introduction of realistic intershell abundances, this approach follows that discussed by Saio & Jeffery (2002), which failed to explain the oxygen abundances without recourse to an *ad hoc* argument. Following discoveries of a large  $^{18}\text{O}$  excess in several RCB and HdC stars (Clayton et al. 2007; García-Hernández et al. 2009), the models for COWDs used by Saio & Jeffery (2002) were re-examined and found to contain a substantial pocket of  $^{18}\text{O}$  at the interface between the CO-core and the He intershell, as well as a reservoir of  $^{22}\text{Ne}$  in the CO-core.

The effective mass and composition of this pocket, as it would contribute to the merged white dwarf is not well constrained by the models we have available. For example, as the star leaves the AGB, the mass of this  $^{18}\text{O}$  pocket may be some  $3.10^{-4} M_{\odot}$ . Subsequent steady He-burning in the post-AGB phase (Fig. 4) produces an  $^{18}\text{O}$  pocket in the pre-merger white dwarf of  $\approx 0.008 M_{\odot}$  (FWHM) having a mean  $^{18}\text{O}$  abundance  $\beta_{^{18}\text{O}:\text{CO}} \approx 0.01$ .

In the models of Saio & Jeffery (2002), this pocket is destroyed when the pocket is reheated by the post-merger accretion-driven helium flash; a new but smaller pocket is established at the outer edge of the newly established He-burning shell. However, if the  $^{18}\text{O}$  pocket or material from deeper in the CO core is mixed during the merger, it may survive. Recalling that there is insufficient carbon in the post-AGB intershell to account for all the carbon observed in EHe and RCB stars, it is highly plausible that any carbon mixed into the merger-product envelope from the CO core will be accompanied by  $^{18}\text{O}$ . This will be diluted by additional  $^{12}\text{C}$  and  $^{16}\text{O}$  if the mixing penetrates significantly beyond the  $^{18}\text{O}$  pocket.

We have therefore incorporated the outer layers of the CO core more realistically. The distribution with mass of  $^4\text{He}$ ,  $^{12}\text{C}$ ,  $^{14}\text{N}$ ,  $^{16}\text{O}$ ,  $^{18}\text{O}$  and  $^{22}\text{Ne}$  is assumed to resemble that of the  $0.60 M_{\odot}$  pre white dwarf shown in Fig. 4, where a core mass of  $0.58 M_{\odot}$  is defined by the point where the carbon and helium abundances are approximately equal. This composition distribution can be applied to COWD cores of different mass ( $m_{\text{CO:CO}}$ ) by scaling its thickness inversely as  $(0.58/m_{\text{CO:CO}})^4$  (this scaling also approximately reproduces the  $m_{\text{He:CO}} - m_{\text{CO:CO}}$  relation implied by Fig. 3).

The abundances of  $^{14}\text{N}$ ,  $^{18}\text{O}$  and  $^{22}\text{Ne}$  may be scaled with metallicity  $Z$ , since  $^{14}\text{N}$  derives mainly from the initial metallicity, and  $^{18}\text{O}$  and  $^{22}\text{Ne}$  are mainly formed from  $\alpha$  captures on  $^{14}\text{N}$ .

To explore the consequences of varying the  $^{12}\text{C}:^{16}\text{O}$  ratio in the outer core, the factor  $f_{\text{CO}}$  can be used to force a rescaling of these two species. The model shown in Fig. 4 has  $f_{\text{CO}} = 0.8$ , but our AGB models suggest  $f_{\text{CO}} = 0.5$ , probably reflecting differences in the adopted  $^{12}\text{C}(\alpha, \gamma)^{16}\text{O}$  rate.

A parameter  $\alpha_{\text{mix}}$  represents the mass within the boundary layer which is mixed into the merged envelope. Formally, if  $\beta(m_r)$  represents the distribution of mass fraction with mass inside the star ( $m_r$ ), we compute

$$\beta_{i:\text{CO:CO}} = \int_{m_i}^{m_o} \beta_{i:\text{CO:CO}}(m_r) dm_r / \int_{m_i}^{m_o} dm_r \quad (33)$$

for  $i$  corresponding to  $^{12}\text{C}$ ,  $^{14}\text{N}$ ,  $^{16}\text{O}$ ,  $^{18}\text{O}$  and  $^{22}\text{Ne}$ . The mass limits are given by

$$m_o = m_{\text{CO:CO}} + m_{\text{sh}}, \quad (34)$$

$$m_i = m_o - \alpha_{\text{mix}} m_{\text{sh}}, \quad (35)$$

$$m_{\text{sh}} = (0.12/m_{\text{CO:CO}})^4. \quad (36)$$

The shell mass  $m_{\text{sh}}$  characterises the scaled shell thickness corresponding to  $0.12 M_{\odot}$  in the  $0.60 M_{\odot}$  pre-WD model.

Thus  $\alpha_{\text{mix}} = 0$  means that no carbon-enriched material from the boundary layer is mixed.  $\alpha_{\text{mix}} = 1$  implies that all material down to the point where the carbon and helium abundances are equal is mixed.  $\alpha_{\text{mix}} = 2$  means that the mixed layer reaches the region where  $^{22}\text{Ne}$  and  $^{16}\text{O}$  are abundant.

Other  $\beta_{i:\text{CO:CO}}$  are as given previously, except

$$\beta_{\text{He:CO:CO}} = 1 - \sum_i \beta_{i:\text{CO:CO}}, \quad (37)$$

since this layer includes some helium from the base of the helium layer. The layer masses  $m_{jk}$  are adjusted to take the blurring of the carbon-helium layer boundary into account.

#### 4.2.4 Final abundances

The ingredients of our model thus comprise five layers of material with masses  $m_{jk}$ , each having a representative composition  $\beta_{ijk}$  defined by current stellar evolution theory. Assuming our primary assertion that all of these layers are fully mixed during the merger, and that no further nucleosynthesis affects the apparent surface composition of the merged product, then the latter is simply represented by

$$\beta_i = \sum_{jk} m_{jk} \beta_{ijk} / \sum_{jk} m_{jk} \quad (38)$$

For comparison with observation, these abundances can be transformed to units more familiar in observational studies. Recall that mass fraction  $\beta$  is defined in terms of number fraction  $n$ :

$$\beta_i = n_i \mu_i / \sum_i n_i \mu_i \quad (39)$$

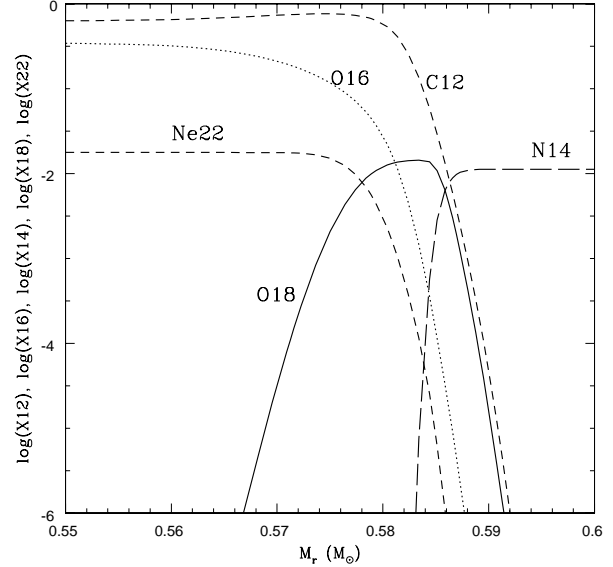


**Figure 4.** The distribution of various elements by mass fraction in the outer layers of a  $0.6 M_{\odot}$  post-AGB star evolving towards the “knee” of the white dwarf sequence.

whence

$$\epsilon_i \equiv \log n_i = \log \frac{\beta_i}{\mu_i} + \log \sum_i \mu_i n_i, \quad (40)$$

$$= \log \frac{\beta_i}{\mu_i} + C' \quad (41)$$

$$C' = \log \sum_i n_i \mu_i - C \quad (42)$$

$$[X] = \epsilon_i - \epsilon_{i\odot}, \quad (43)$$

where  $n_i$  are the relative abundances of species  $i$  by number ( $\sum n_i = 1$ ), and  $C$  is defined by Eq. 2.

### 4.3 Nucleosynthesis during a hot merger

In the *cold* merger model, the chemical composition of the HeWD is assumed to be unchanged during a merger with a COWD. However, SPH calculations indicate that some of this material may briefly reach temperatures of  $6 \times 10^8 \text{K}$  or more (Guerrero et al. 2004; Yoon et al. 2007; Lorén-Aguilar et al. 2009), and that some nucleosynthesis of  $\alpha$ -rich material will occur. Yoon et al. (2007) and Lorén-Aguilar et al. (2009) demonstrate how the disrupted material forms a relatively unprocessed disk containing slightly more than half of the HeWD, and a heavily processed corona containing the remainder. How the disk and corona are subsequently assimilated into the merged star, and what mixing processes occur, is not yet obvious. The simplest assumption is that turbulent mixing during the merger, and nuclear- and surface-driven convection following stable helium-shell ignition will completely mix both disk and corona with material from the intershell of the COWD.

This process can be incorporated into our model. Lorén-Aguilar et al. (2009) (Tables 1 and 2) give sample masses and chemistries for the disk and corona in the cases of a  $0.3 + 0.5 M_{\odot}$  and a  $0.4 + 0.8 M_{\odot}$  He+CO WD merger.

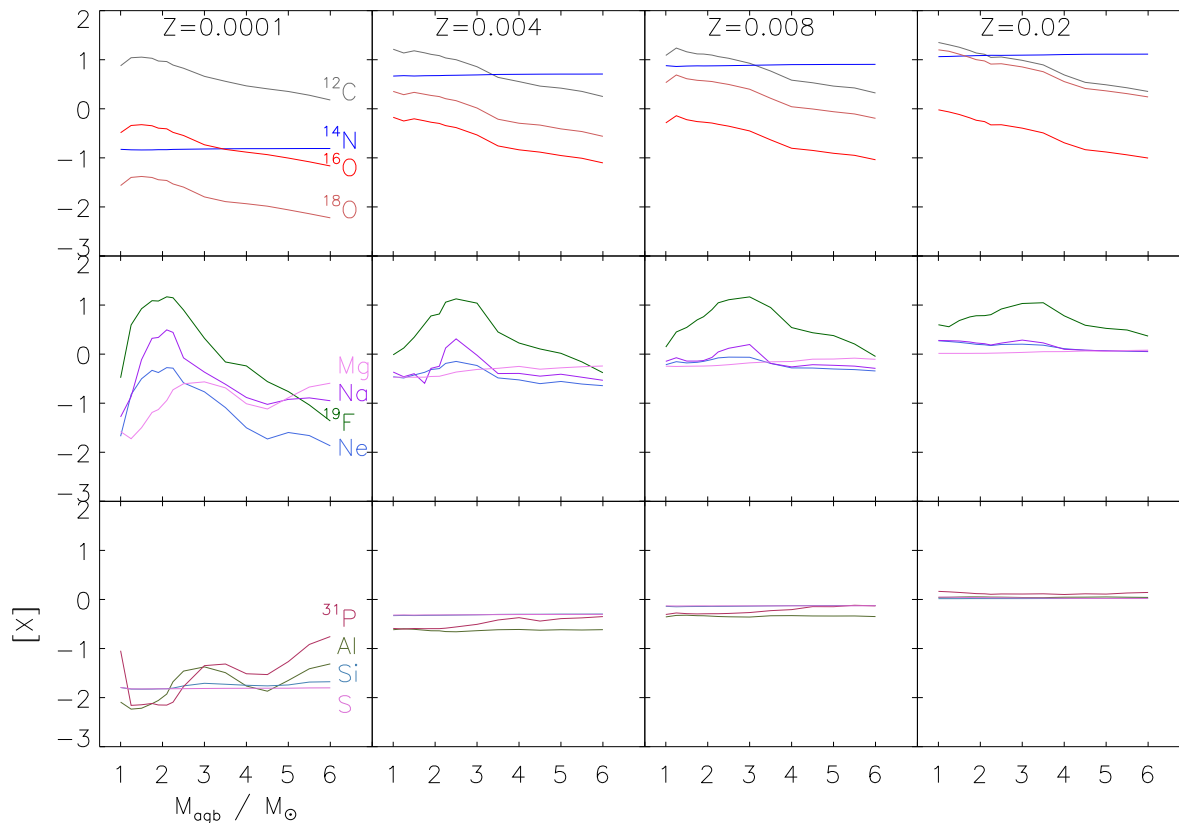


**Figure 5.** Surface abundances (log number relative to solar) predicted from our simple recipe for a merged white dwarf as a function of initial mass for the COWD ( $m_{\text{agb}}$ ) for four values of initial metallicity ( $Z$ ). Elements and isotopes are coded by colour (shade of grey) and labelled in the left column.

Using  $m_{\text{He:He}}$  from Eq. 12 and interpolating we obtain  $m_{\text{disk:He}}$  and  $m_{\text{corona:He}}$  for  $0.3 < m_{\text{He:He}} < 0.4$  (we do not extrapolate), and also chemistries for the same material. Lorén-Aguilar et al. (2009) compute models starting with a pure helium mixture for the HeWD and a carbon-oxygen mixture for the CO white dwarf, so we arbitrarily impose a  $Z$ -dependent lower limit on individual abundances in the disk and corona as given by the prescription for the *cold* merger. We note that contamination by a small amount of hydrogen and other metals will profoundly affect the predicted *hot merger* nucleosynthesis, but we have no data on how this might affect current results.

## 5 ELEMENTAL YIELDS

### 5.1 Cold merger

The predicted surface composition following the *cold* merger of a He+CO WD with some core mixing is illustrated in Figs. 5, 6, and 7.

Fig. 5 shows the surface abundance of each species relative to the solar surface abundance as a function of  $m_{\text{agb}}$  (the progenitor mass of the AGB star) for each of four initial metallicities  $Z$ . This figure demonstrates that several species show high yields roughly independent of  $m_{\text{agb}}$ .  $^{12}\text{C}$  and  $^{18}\text{O}$  show uniformly high yields as defined by the core mixing parameters. The  $^{16}\text{O}$  yield is proportional to the  $^{12}\text{C}$  yield; effectively determined by the  $^{16}\text{O}/^{12}\text{C}$  ratio in the

outer edge of the core. The  $^{14}\text{N}$  yield is proportional to  $Z$  as expected; it is determined by the initial CNO abundance. Note how the yields of  $^{19}\text{F}$ , Na and Ne are strongly peaked in the interval  $1.5 < m_{\text{agb}}/M_{\odot} < 3$ , whilst  $^{31}\text{P}$  and Al are only significantly enhanced ( $\geq 0.5$  dex) toward higher masses ( $m_{\text{agb}} > 2 M_{\odot}$ ). These yields reflect the AGB intershell nucleosynthesis. Meanwhile  $^{12}\text{C}$ ,  $^{14}\text{N}$  and  $^{18}\text{O}$  are enhanced almost uniformly with  $m_{\text{agb}}$  and  $Z$ , effectively as the model was designed to deliver.

Fig. 6 shows these same data rearranged as a function of initial metallicity  $[\text{Fe}] \equiv \log Z/Z_{\odot}$  for four representative masses  $m_{\text{agb}} = 1, 1.9, 3$  and  $5 M_{\odot}$ . They are plotted together with the observed abundance data in exactly the same way as in Fig. 1. Since we have only used two AGB models for the s-process elements, a single broken line represents the provisional prediction for  $m_{\text{agb}} \approx 3 M_{\odot}$ . Several correlations are noteworthy.

### 5.2 Cold merger: individual elements

*Carbon:* the model carbon enhancement was chosen to match the abundances measured in EHe stars by adjusting the degree of core mixing. The EHe carbon measurements are probably more representative than the RCB measurements because of the “carbon problem” referred to earlier. The EHe star data show a significant scatter. Allowing  $\alpha_{\text{mix}}$  to vary by  $\pm 1$  gives results still broadly consistent with the observed carbon (and oxygen) abundances.

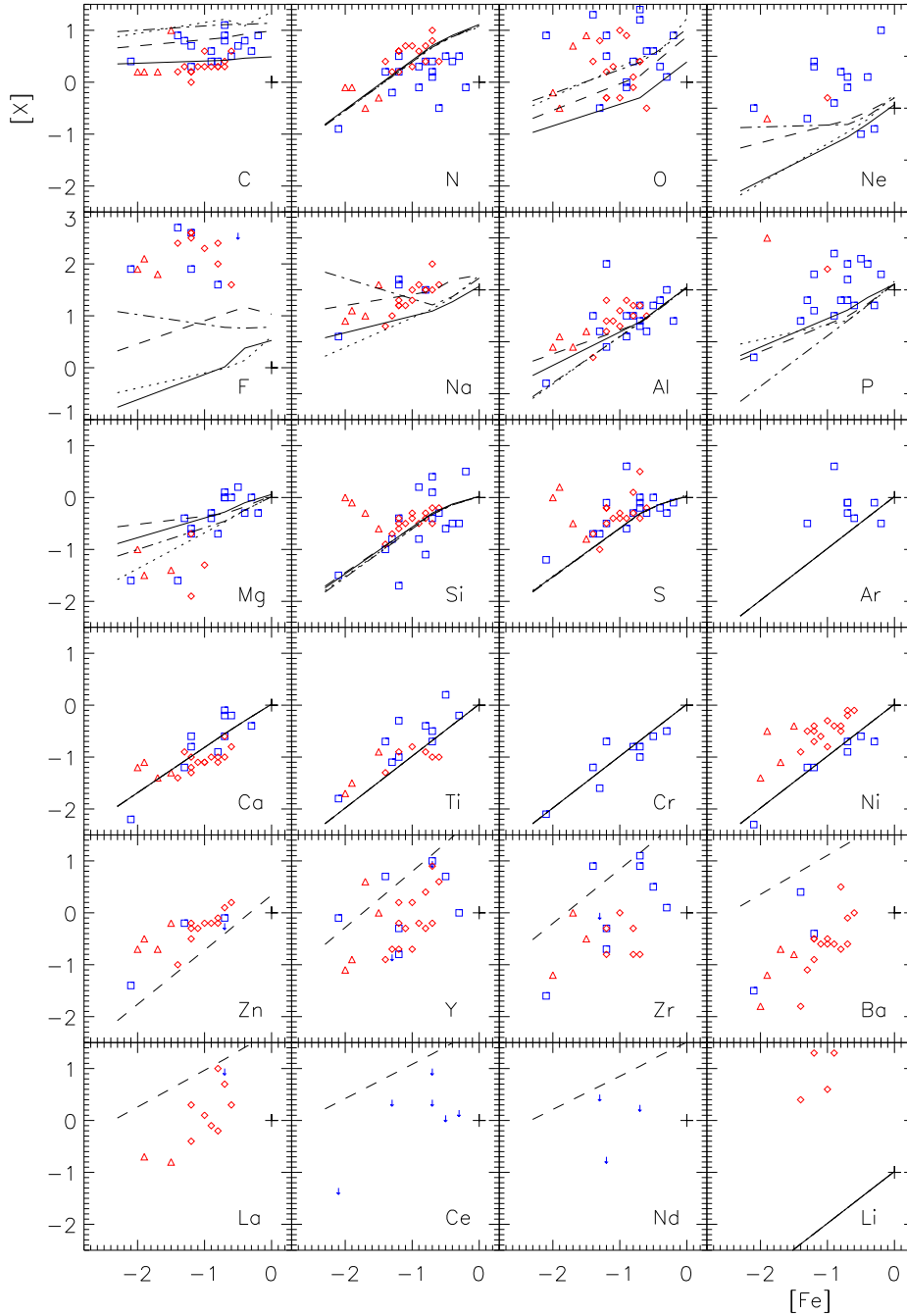


**Figure 6.** As Fig. 1. The over-plotted lines represent the surface abundances predicted from a cold CO+He white dwarf merger. Predictions for four initial masses are shown:  $m_{\text{agb}}/M_{\odot} = 1$  (dotted), 1.9 (dash-dot), 3 (dashed) and 5 (solid). Two or more lines are coincident in several panels, especially where only a single solid line appears. The very provisional result for s-process elements (see §4.2.2) is represented by a single dashed line. In this simulation, most of the the carbon and oxygen are dredged from the carbon/helium boundary layer at the top of CO core ( $\alpha_{\text{mix}} = 3$ ,  $f_{\text{CO}} = 0.8$ ).

*Nitrogen:* a generally excellent correlation with the observations, supporting the basic assumption that the surfaces of EHe and RCB stars are primarily CNO-processed helium.

*Oxygen:* a modest  $^{18}\text{O}$  pocket at the helium-carbon boundary in the CO white dwarf progenitor may explain the most extreme oxygen abundances seen in metal-rich EHe and

RCB stars, providing this layer is mixed during or immediately after the merger. Note, however, that oxygen isotope ratios are known for only a few RCB stars and for no EHe stars, that  $^{18}\text{O}$  may be destroyed by high temperatures during the merger. An alternative is that the  $^{16}\text{O}:^{12}\text{C}$  ratio in the outer core is approximately unity or more.

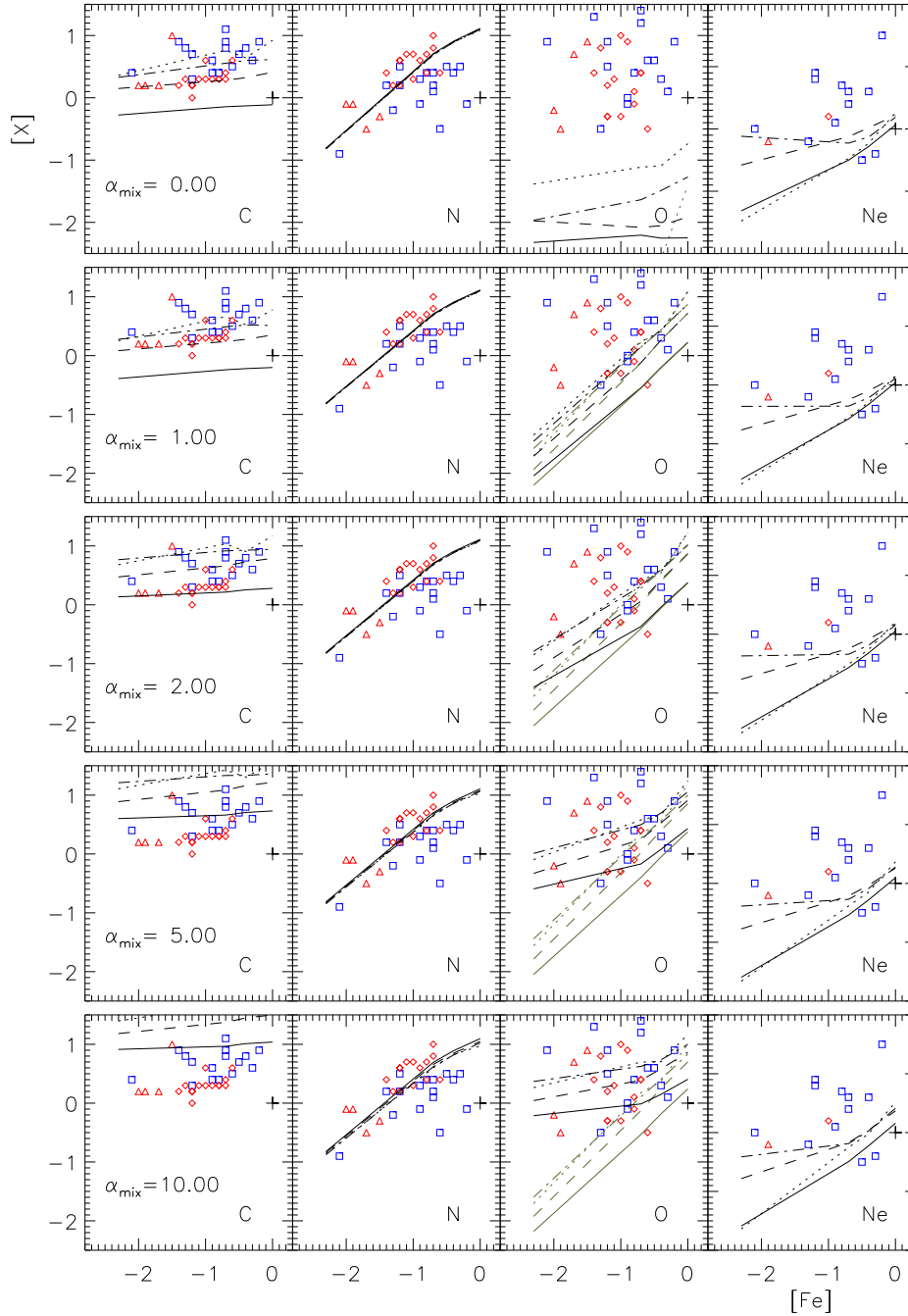


**Figure 7.** As the top 4 panels of Fig. 1 repeated with different values for the core-shell boundary mixing parameter  $\alpha_{\text{mix}}$ . The top row represents the inclusion of *no* helium-depleted material from the boundary layer. The second row represents mixing down to a point where carbon and helium abundances are equal. The bottom three rows represent increasingly deep mixing into material stratified as in Fig. 4;  $\alpha_{\text{mix}} = 1$  includes 50% of the  $^{18}\text{O}$  pocket. The contribution of  $^{18}\text{O}$  to the total oxygen abundance is shown in olive (grey).

*Neon:* intermediate-mass models ( $1.9, 3 M_{\odot}$ ) show significant enhancements of neon, formed primarily in the intershell of the AGB precursor. These match a few of the observed neon abundances, but the very high abundances measured in at least seven EHe stars are not yet explained by this model.

*Fluorine:* as in the case of neon, a significant  $^{19}\text{F}$  excess is generated in the intershell of the intermediate-mass models

( $1.9, 3 M_{\odot}$ ), suggesting a likely source for the observed excess. However, the predictions remain  $\approx 1$  dex smaller than the measurements. However,  $^{18}\text{O}$  from the C/He boundary in the COWD provides an ample reservoir for the prompt production of  $^{19}\text{F}$  if it is sufficiently heated, together with protons, during the merger; thus the model prediction represents a strict lower limit.

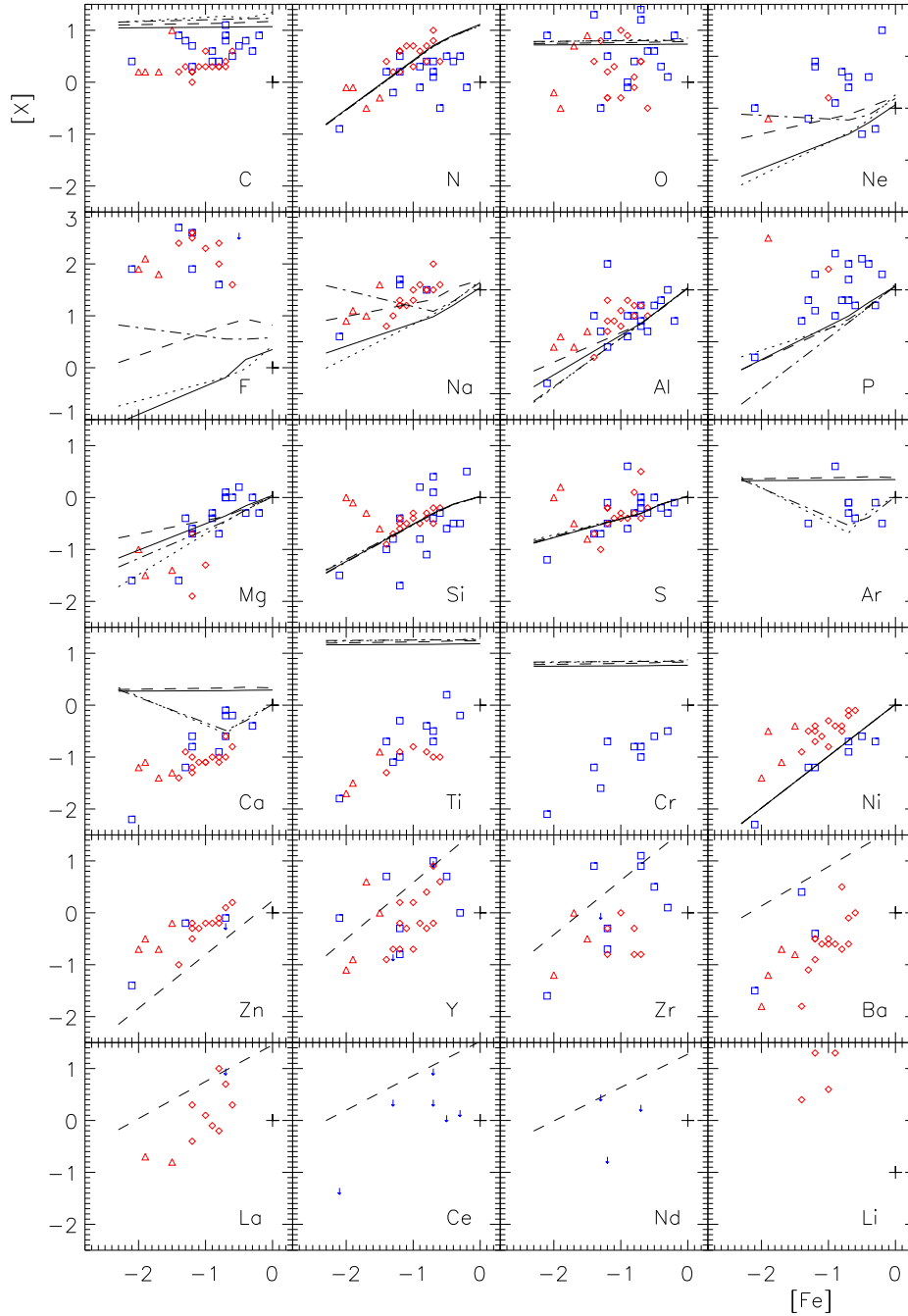


**Figure 8.** As Fig. 6 except that the over-plotted lines represent the surface abundances predicted from a hot CO+He white dwarf merger and include no mixing with the CO core ( $\alpha_{\text{mix}} = 0$ ). Nucleosynthesis in the disrupted He-WD during the merger is interpolated between results for a  $0.3 + 0.5M_{\odot}$  and a  $0.4 + 0.8M_{\odot}$  merger (Lorén-Aguilar et al. 2009). The predictions for Ti and Cr are based on the model for a  $0.3 + 0.5M_{\odot}$  merger only.

*Sodium, Aluminium, and Magnesium:* the recipe predicts some enhancement of these light elements over their initial values, particularly at low- $Z$  for aluminium and magnesium. These predicted abundances are broadly consistent with the measurements for EHe and RCB stars in the case of sodium and aluminium. The under abundance of magnesium in both EHe and RCB stars at low- $Z$  requires further investigation.

*Phosphorus:* a primary motivation for this investigation, the recipe shows that  $^{31}\text{P}$  generated in an AGB intershell can propagate to the surface of a subsequent white dwarf merger. The recipe only predicts significant overabundances at low- $Z$ . Although this is consistent with one low- $Z$  phosphorus measurement and eight high- $Z$  EHe measurements, the

recipe does it not explain a  $\geq 1$  dex overabundances observed in eight other high- $Z$  and one low- $Z$  measurements. *Silicon, Sulphur, Argon, Calcium, Titanium, Chromium, and Nickel*: the *cold* merger recipe predicts negligible (silicon) or *no enhancement* beyond that expected from the enhancement of  $\alpha$  elements in low- $Z$  progenitors. The observations are *broadly* consistent with the recipe predictions for all of these elements. A number of stars with up to 1 dex enhancements of silicon, sulphur and/or argon demand further attention. In particular, the observed scatter of  $\pm 1$  dex in silicon is not obviously explained by this recipe.

*s-process*: our provisional predictions for the s-process elements zinc, yttrium, zirconium, barium, lanthanum, cerium and neodymium indicate a substantial excess is expected in all cases except zinc. The predictions are all in excess of the mean trend of the observed abundances (or their upper limits). For Y, Zr, and La, they are not in excess of the upper limit of the observed abundances. Given the small number of models available, and the probability that other factors will affect the observed distribution of s-process abundances, these results are inconclusive, but encouraging.

It will be noted (*e.g.* from Fig. 6) that the predicted excesses of certain elements are strong functions of the progenitor mass ( $m_{\text{agb}}$ ) and metallicity. Notable amongst these are neon, fluorine, sodium, and magnesium. An early objective of this investigation was to determine whether the observed abundances placed any firm constraints on the progenitor mass. For example, significant excesses (which are observed) in neon, fluorine, and sodium are predicted for  $1.9 < m_{\text{agb}}/M_{\odot} < 3$ , whilst an excess of magnesium (which is not observed) is only predicted for  $m_{\text{agb}}/M_{\odot} \geq 3$ . The evidence from phosphorus and aluminium remains ambiguous. The suggestion is therefore that the progenitor AGB stars had initial masses in the range  $1.9 < m_{\text{agb}}/M_{\odot} < 3$ . This suggestion assumes that the binary components evolved essentially as single stars up to the AGB, plausible if the first common-envelope phase required to produce the short-period double-white-dwarf binary occurred after the more massive star reached the AGB.

### 5.3 Cold merger: core mixing

Figure 7 illustrates the effect of  $\alpha_{\text{mix}}$  on the abundances of the principal elements C, N, O and Ne, and also shows the contribution of  $^{18}\text{O}$  to the total oxygen abundance. It must be noted that these results depend strongly on the composition profile at the carbon-helium boundary, and in particular on the  $^{16}\text{O}:^{12}\text{C}$  ratio immediately below the boundary layer. The intent is to demonstrate the effect of increasing the depth of mixing on the final model abundances.

$\alpha_{\text{mix}} = 0$ : the first row of Fig. 7 represents the case of no contribution from the boundary layer, oxygen completely fails to match the observed abundances of EHe and RCrB stars. There may be sufficient carbon in the intershell of intermediate mass ( $m_{\text{agb}} \approx 2-3 M_{\odot}$ ) to reproduce the lower envelope of the carbon and neon abundances, but not the full range.

$\alpha_{\text{mix}} = 1$ : the second row of Fig. 7, representing mixing down to the helium/carbon equilibrium point, has similar results for carbon, nitrogen and neon, but immediately shows much more oxygen at high  $Z$ . This oxygen is almost entirely  $^{18}\text{O}$  (assuming that it survives the actual merger). The care-

ful reader will note that the carbon abundances are slightly depressed compared with  $\alpha_{\text{mix}} = 0$ ; this is due to a mismatch between the intershell carbon abundances given in the Karakas (2010) models and the abundances in the pre-WD model shown in Fig. 4.

$\alpha_{\text{mix}} = 2$ : slightly deeper mixing substantially improves the carbon result without much change to other elements.

$\alpha_{\text{mix}} \gg 2$ : with very deep mixing, the models start to show too much carbon. Oxygen is increasingly composed of  $^{16}\text{O}$  and becomes independent of  $Z$ , although at high  $Z$ ,  $^{18}\text{O}$  remains a significant constituent. The contribution of  $^{22}\text{Ne}$  from the core has an almost negligible impact, even in high- $Z$  models.

As noted above, a shift in the  $^{12}\text{C}/^{16}\text{O}$  ratio immediately below the boundary layer alters the chemical balance. By setting  $f_{\text{CO}} = 0.3$ , it was possible to obtain a good correspondence between model and observation for C, N, O, and the  $^{18}\text{O}/^{16}\text{O}$  ratio at the same time (not shown). However, the value of  $f_{\text{CO}}$  required is unjustifiably smaller than the value of 0.5 obtained in the Karakas (2010) models. The prospects for neon seem less good; its abundance is primarily limited by the original CNO abundance.

Further investigation of the chemical structure of white dwarf models derived from realistic AGB calculations will indicate whether the *cold* merger model stands up to scrutiny. Meanwhile, Fig. 7 suggests that  $\alpha_{\text{mix}} = 3$  is satisfactory for the time being. Moreover, by indicating how much material from below the C/He boundary must have been mixed, the value of  $\alpha_{\text{mix}}$  may also tell us something about the (*cold*) merger process itself.

### 5.4 Hot merger

Figure 8 shows the chemical yields predicted by this simplification of the *hot merger* model. In this case, there is *no* contribution to the carbon and oxygen from mixing with the He/CO boundary layer from the COWD. *All* of the excess carbon and oxygen comes from nucleosynthesis during the merger.

The calculations by Lorén-Aguilar et al. (2009) indicate significant production of iron, nickel and zinc, and very large quantities of argon, calcium, titanium and chromium produced by  $\alpha$ -capture reactions in the hot corona, especially towards the upper limit of the He-WD mass range ( $0.4 M_{\odot}$ ). At this limit, the titanium and chromium yields are so high as to be off scale in Figure 8; thus we have restricted the nucleosynthesis of these two elements to the lower limit of their predicted range. The theoretical yields of iron, nickel and zinc are below the threshold defined by the initial metallicity and hence have no effect on the final abundances (Fig. 8) compared with the model for the *cold* merger (Fig. 6).

The surface abundances following a *hot merger* as predicted by the *simple recipe* are shown in Fig. 8. Recall that mixing at the carbon-helium boundary is switched off in this case. The predictions are complicated by having very few models amongst which to interpolate, making the  $Z$ -distribution of elements strongly affected by merger nucleosynthesis indicative rather realistic (*cf.* argon and calcium) *Carbon and Oxygen.*, all surface carbon and oxygen is produced by nucleosynthesis during the hot merger. The quantities are comparable with those from the *cold* merger, but

in this case *no* parameters were tuned to achieve the correct outcome.

*Sulphur*: additional sulphur produced in the *hot merger* provides a better fit to the observations than in the *cold* merger.

*Argon*: there is weak evidence of an argon excess in some EHes; this provides some support for its formation in a hot merger, possibly in higher-mass mergers ( $m_{\text{agb}} > 2 M_{\odot}$ ).

*Calcium, Titanium, and Chromium*: the SPH merger calculations of Lorén-Aguilar et al. (2009), combined with the merger recipe described here, predict very high surface abundances of these three elements in nearly all cases. There is no observational evidence that any of these elements is significantly overabundant in any EHe or RCB star analysed to date. If EHes and RCBs are formed in a merger, there is no evidence that reactions leading to the production of calcium, titanium, or chromium operate during the merger process. This places strong constraints on temperatures and timescale of the *hot merger*.

*Fluorine*: although not treated in the models of Lorén-Aguilar et al. (2009), any  $^{18}\text{O}$  produced or mixed into the heated material will be at least partially burnt to make  $^{19}\text{F}$ , providing the temperature does not significantly exceed  $3.10^8$  K, where the F will subsequently be destroyed by  $\alpha$  captures. Hence the presence of any  $^{18}\text{O}$  will almost inevitably result in an excess of  $^{19}\text{F}$ .

*Lithium*: Li should be destroyed during a hot merger. Lorén-Aguilar et al. (2009) do not include Li, so predictions for Li are not shown in Fig. 8.

### 5.5 Uncertainties

The obvious question is what confidence can be placed on using a simple recipe to predict the outcome of a complicated process? For any element which is produced outside the standard hydrogen and helium-burning reactions (*e.g.* s-process elements in the AGB precursor), the major impact on the final surface yield is the degree of dilution by the accreted helium white dwarf. In our recipe this is primarily constrained by the minimum white dwarf mass for a conservative merger. Were  $m_{\text{He}}$  to exceed this value, the predicted excesses would be reduced. This does not help to explain neon, fluorine or phosphorus in EHes. Were the merger to be non-conservative (efficiency  $\alpha < 1$ ), yields might increase by factors  $1/\alpha$ . SPH calculations support  $\alpha = 1$ . Efficiencies  $\alpha \ll 1$  would be surprising. Explaining neon, fluorine and phosphorus would require  $\alpha < 0.1$ .

The neglect of specific mixing processes or individual reactions in the stellar evolution models will impact on the recipe predictions. For example, the intershell compositions from Karakas (2010) were computed without the addition of a  $^{13}\text{C}$  pocket. This pocket is thought to form by the mixing of protons from the H-rich envelope into the intershell during the deepest extent of a third dredge-up episode. These protons are quickly captured by the abundant  $^{12}\text{C}$  resulting in the formation of a  $^{13}\text{C}$  pocket. Here, neutrons are liberated by the reaction  $^{13}\text{C}(\alpha, n)^{16}\text{O}$  during the interpulse. Note that in most calculations the  $^{13}\text{C}$  pocket is added artificially or induced through the inclusion of convective overshoot (*e.g.* Herwig 2000). Whilst  $^{13}\text{C}$  pockets facilitate the formation of s-process elements, they are also important for enhancing the abundance of some lighter elements including  $^{19}\text{F}$ ,  $^{22}\text{Ne}$ , and  $^{23}\text{Na}$  (Lugaro et al. 2004; Karakas 2010).

Legitimate questions concern the core and shell masses for the AGB stars, the yields obtained in the AGB intershell nucleosynthesis and in the hot merger nucleosynthesis. For example, how sensitive are the masses adopted here to the microphysics, *e.g.* convection, rotation, mass-loss and/or mass transfer? Since the model abundances are computed for CO+He WDs with  $q = q_{\text{crit}}$ , would additional dilution produced  $q > q_{\text{crit}}$  seriously compromise the results? If mass transfer occurs before AGB evolution is complete, or even before the star reaches the AGB, are the intershell-yield versus initial-mass relations still acceptable? What would the hot-merger nuclear-hydro calculations look like with more realistic networks and initial composition? We have discussed the question of the chemical structure of COWDs, particularly at the C/He boundary layer. Additional calculations for *hot mergers* with more extensive reaction networks and robust starting mixtures are also urgently needed.

## 6 CONCLUSION

The object of this paper was to clarify the surface abundances which might arise under conservative assumptions for the merger of a helium white dwarf with a carbon-oxygen white dwarf, and to compare these with observed abundance anomalies for extreme helium and R Coronae Borealis stars. We have collated the observational data describing the surface abundances for the latter, and presented it, element by element, in a way that demonstrates any current excess over the progenitor composition. We have discussed the background to the physics of binary white dwarf mergers and their association with the formation of extreme helium stars and R Coronae Borealis stars. We have developed a more elaborate version of the *simple recipe* used to estimate surface abundances in previous discussions of this question (Saio & Jeffery 2002; Pandey et al. 2006). We have incorporated state-of-the-art calculations of the masses and light-element composition of AGB intershell regions (Karakas 2010). We have made allowance for the existence of an  $^{18}\text{O}$  pocket at the outer edge of the CO core. We have considered the difference between a *cold* and a *hot* merger, *i.e.* whether additional nucleosynthesis occurs during the destruction of the helium white dwarf.

Both models successfully match, or can be made to match, the observed surface abundances of carbon, nitrogen, and oxygen. The excess nitrogen comes primarily from the helium white dwarf as the residue of CNO-processed carbon and oxygen. In the case of the *cold* merger model, the excess carbon and oxygen comes from the carbon-helium boundary of the carbon-oxygen white dwarf. A substantial fraction of oxygen probably takes the form of  $^{18}\text{O}$  from a pocket just beneath this boundary, but  $^{16}\text{O}$  dredged from deeper layers will also be present. In the case of the *hot* merger model, the excess carbon and oxygen can be produced during the merger. It is possible that the observed excess comes from both sources.

Both models predict up to 1 dex enhancements of  $^{19}\text{F}$  and  $^{31}\text{P}$ , but not enough to match the observed overabundances of fluorine and phosphorus. These elements come from the AGB intershell. An examination of mixing at the carbon/helium boundary of the COWD suggests that ob-

served neon may come from the outer part of the carbon/oxygen core.

Both models predict modest overabundances of sodium, aluminium and magnesium, particularly at low metallicity. These broadly match the observed abundance distributions in sodium and aluminium. Magnesium is not observed in excess at low- $Z$ .

The *hot* merger model currently predicts overabundances of calcium, titanium and chromium which are not observed. The model overabundance of argon is roughly consistent with available measurements, suggesting that argon might be produced during hot merger nucleosynthesis. We do not yet have AGB intershell yields for argon, which would affect the *cold* merger predictions.

We still require state-of-the-art data for s-process yields in AGB intershell.

Overall, the majority of species observed to be overabundant in EHe and RCB stars are found to be enhanced in reasonable quantity in one or other of the white dwarfs prior to merger. In other words, additional nucleosynthesis during a merger solves very few problems, although that does not mean that it does not happen.

## ACKNOWLEDGMENTS

The authors gratefully acknowledge Detlef Schönberner, Ulrich Heber, David Lambert, Gajendra Pandey, Kameswara Rao, and Martin Asplund and the late Philip Hill for their inspirational efforts in measuring stellar abundances over 50 years. They also thank John Lattanzio, Maria Lugaro and Simon Campbell for discussions on AGB nuclear networks and particularly the nuclear origin of phosphorus in EHe stars.

The Armagh Observatory is funded by direct grant from the Northern Ireland Dept of Culture Arts and Leisure.

CSJ acknowledges an Australian National University visiting fellowship.

## REFERENCES

- Abia C., Cunha K., Cristallo S., de Laverny P., Domínguez I., Eriksson K., Gialanella L., Hinkle K., Imbriani G., Recio-Blanco A., Smith V. V., Straniero O., Wahlin R., 2010, *ApJ*, 715, L94
- Anders E., Grevesse N., 1989, *Geochim. Cosmochim. Acta*, 53, 197
- Asplund M., Gustafsson B., Kiselman D., Eriksson K., 1997, *A&A*, 318, 521
- Asplund M., Gustafsson B., Lambert D. L., Rao N. K., 2000, *A&A*, 353, 287
- Behara N. T., Jeffery C. S., 2006, *A&A*, 451, 643
- Benz W., Cameron A. G. W., Press W. H., Bowers R. L., 1990, *ApJ*, 348, 647
- Brown T. M., Sweigart A. V., Lanz T., Landsman W. B., Hubeny I., 2001, *ApJ*, 562, 368
- Busso G., Moehler S., Zoccali M., Heber U., Yi S. K., 2005, *ApJ*, 633, L29
- Clayton G. C., 1996, *PASP*, 108, 225
- Clayton G. C., Geballe T. R., Herwig F., Fryer C., Asplund M., 2007, *ApJ*, 662, 1220
- Clayton G. C., Herwig F., Geballe T. R., Asplund M., Tenenbaum E. D., Engelbracht C. W., Gordon K. D., 2005, *ApJ*, 623, L141
- Clayton G. C., Kerber F., Pirzkal N., De Marco O., Crowther P. A., Fedrow J. M., 2006, *ApJ*, 646, L69
- Cottrell P. L., Lambert D. L., 1982, *ApJ*, 261, 595
- Driebe T., Schönberner D., Blöcker T., Herwig F., 1998, *A&A*, 339, 123
- Drilling J. S., Jeffery C. S., Heber U., 1998, *A&A*, 329, 1019
- García-Hernández D. A., Hinkle K. H., Lambert D. L., Eriksson K., 2009, *ApJ*, 696, 1733
- García-Hernández D. A., Lambert D. L., Rao N. K., Hinkle K. H., Eriksson K., 2010, *arXiv*, 1003, 2901v1
- Goswami A., Prantzos N., 2000, *A&A*, 359, 191
- Gurrero J., García-Berro E., Isern J., 2004, *A&A*, 413, 257
- Han Z., 1998, *MNRAS*, 296, 1019
- Han Z., Webbink R. F., 1999, *A&A*, 349, L17
- Harrison P. M., Jeffery C. S., 1997, *A&A*, 323, 177
- Heber U., 1983, *A&A*, 118, 39
- Herwig F., 2000, *A&A*, 360, 952
- Hunger K., Klinglesmith D., 1969, *ApJ*, 157, 721
- Iben Jr. I., Kaler J. B., Truran J. W., Renzini A., 1983, *ApJ*, 264, 605
- Iben Jr. I., Tutukov A. V., 1984, *ApJS*, 54, 335
- Iben Jr. I., Tutukov A. V., 1985, *ApJS*, 58, 661
- Iben I. J., 1990, *ApJ*, 353, 215
- Iben I. J., Tutukov A. V., Yungelson L. R., 1996, *ApJ*, 456, 750
- Jeffery C. S., 1988, *MNRAS*, 235, 1287
- Jeffery C. S., 1993, *A&A*, 279, 188
- Jeffery C. S., 1996, in Jeffery C. S., Heber U., eds, *Hydrogen Deficient Stars Vol. 96 of Astronomical Society of the Pacific Conference Series, Surface properties of extreme helium stars*. p. 152
- Jeffery C. S., 1998, *MNRAS*, 294, 391
- Jeffery C. S., 2008, in Werner A., Rauch T., eds, *Hydrogen-Deficient Stars Vol. 391 of Astronomical Society of the Pacific Conference Series, Extreme Helium Stars: A Decade of Progress*. p. 53
- Jeffery C. S., Harrison P. M., 1997, *A&A*, 323, 393
- Jeffery C. S., Heber U., 1992, *A&A*, 260, 133
- Jeffery C. S., Heber U., 1993, *A&A*, 270, 167
- Jeffery C. S., Heber U., Hill P. W., Dreizler S., Drilling J. S., Lawson W. A., Leuhenagen U., Werner K., 1996, in Jeffery C. S., Heber U., eds, *Hydrogen Deficient Stars Vol. 96 of Astronomical Society of the Pacific Conference Series, A catalogue of hydrogen-deficient stars*. p. 471
- Jeffery C. S., Hill P. W., Heber U., 1999, *A&A*, 346, 491
- Jeffery C. S., Woolf V. M., Pollacco D. L., 2001, *A&A*, 376, 497
- Jorissen A., Smith V. V., Lambert D. L., 1992, *A&A*, 261, 164
- Karakas A. I., 2010, *MNRAS*, 403, 1413
- Kaufmann J. P., Schönberner D., 1977, *A&A*, 57, 169
- Kawai Y., H. S., Nomoto K., 1987, *ApJ*, 315, 229
- Kawai Y., Saio H., Nomoto K., 1988, *ApJ*, 328, 207
- Lambert D. L., Rao N. K., 1994, *Journal of Astrophysics and Astronomy*, 15, 47
- Landau L., Lifshitz E., 1958, *The Classical Theory of Fields*. Pergamon, Oxford

- Lee Y., Joo S., Han S., Chung C., Ree C. H., Sohn Y., Kim Y., Yoon S., Yi S. K., Demarque P., 2005, *ApJ*, 621, L57
- Lorén-Aguilar P., Isern J., García-Berro E., 2009, *A&A*, 500, 1193
- Lugaro M., Ugalde C., Karakas A. I., Görres J., Wiescher M., Lattanzio J. C., Cannon R. C., 2004, *ApJ*, 615, 934
- Lynden-Bell D., Pringle J. E., 1974, *MNRAS*, 168, 603
- Lynden-Bell D., Tout C. A., 2001, *ApJ*, 558, 1
- Marsh T. R., 1995, *MNRAS*, 275, L1
- Marsh T. R., Dhillon V. S., Duck S. R., 1995, *MNRAS*, 275, 828
- Maxted P. F. L., Marsh T. R., Moran C. K. J., 2002, *mnras*, 332, 745
- Möller R. U., 1990, Master's thesis, Universität Kiel
- Morales-Rueda L., Marsh T. R., Maxted P. F. L., Nelemans G., Karl C., Napiwotzki R., Moran C. K. J., 2005, *MNRAS*, 359, 648
- Napiwotzki R., Drechsel H., Heber U., Karl C., Pauli E., Christlieb N., Hagen H., Reimers D., Koester D., Moehler S., Homeier D., Leibundgut B., Renzini A., Marsh T. R., Nelemans G., Yungelson L., 2003, in D. de Martino, R. Silvotti, J.-E. Solheim, & R. Kalytis ed., *NATO ASIB Proc. 105: White Dwarfs Search for double degenerate progenitors of supernovae type Ia with SPY*. pp 39–+
- Nather R. E., Robinson E. L., Stover R. J., 1981, *ApJ*, 244, 269
- Nelemans G., Napiwotzki R., Karl C., Marsh T. R., Voss B., Roelofs G., Izzard R. G., Montgomery M., Reerink T., Christlieb N., Reimers D., 2005, *A&A*, 440, 1087
- Nelemans G., Yungelson L. R., Portegies Zwart S. F., Verbunt F., 2001, *A&A*, 365, 491
- Nomoto K., Hashimoto M., 1987, *Ap&SS*, 131, 395
- Nomoto K., Sugimoto D., 1977, *PASJ*, 29, 765
- Pandey G., 2006, *ApJ*, 648, L143
- Pandey G., Kameswara Rao N., Lambert D. L., Jeffery C. S., Asplund M., 2001, *MNRAS*, 324, 937
- Pandey G., Lambert D. L., 2010, *ArXiv e-prints*
- Pandey G., Lambert D. L., Jeffery C. S., Rao N. K., 2006, *ApJ*, 638, 454
- Pandey G., Lambert D. L., Rao N. K., 2008, *ApJ*, 674, 1068
- Pandey G., Lambert D. L., Rao N. K., Gustafsson B., Ryde N., Yong D., 2004, *MNRAS*, 353, 143
- Pandey G., Lambert D. L., Rao N. K., Jeffery C. S., 2004, *ApJ*, 602, L113
- Pandey G., Reddy B. E., 2006, *MNRAS*, 369, 1677
- Pringle J. E., Webbink R. F., 1975, *MNRAS*, 172, 493
- Przybilla N., Butler K., Heber U., Jeffery C. S., 2005, *A&A*, 443, L25
- Rao N. K., Lambert D. L., 1996, in C. S. Jeffery & U. Heber ed., *Hydrogen Deficient Stars Vol. 96 of Astronomical Society of the Pacific Conference Series, Surface composition of the RCB stars - refinement of a few mere facts*. pp 43–+
- Rao N. K., Lambert D. L., 2008, *MNRAS*, 384, 477
- Rich R. M., Salim S., Brinchmann J., Charlot S., Seibert M., Kauffmann G., Lee Y.-W., Yi S. K., Barlow T. A., Bianchi L., more ., 2005, *ApJ*, 619, L107
- Ryde N., Lambert D. L., 2004, *A&A*, 415, 559
- Saffer R. A., Liebert J., Olszewski E. W., 1988, *ApJ*, 334, 947
- Saio H., Jeffery C. S., 2000, *MNRAS*, 313, 671
- Saio H., Jeffery C. S., 2002, *MNRAS*, 333, 121
- Saio H., Nomoto K., 1995, *A&A*, 150, L21
- Saio H., Nomoto K., 1998, *ApJ*, 500, 388
- Saio H., Nomoto K., 2004, *ApJ*, 615, 444
- Schönberner D., 1986, in Hunger K., Schönberner D., Kameswara Rao N., eds, *IAU Colloq. 87: Hydrogen Deficient Stars and Related Objects Vol. 128 of Astrophysics and Space Science Library, Evolutionary status and origin of extremely hydrogen-deficient stars*. pp 471–480
- Segretain L., Chabrier G., Mochkovitch R., 1997, *ApJ*, 481, 355
- Tutukov A. V., Yungelson L. R., 1979, *Acta Astronomica*, 29, 665
- Warner B., 1967, *MNRAS*, 137, 119
- Webbink R. F., 1984, *ApJ*, 277, 355
- Werner K., Herwig F., 2006, *PASP*, 118, 183
- Werner K., Rauch T., Reiff E., Kruk J. W., 2009, *Ap&SS*, 320, 159
- Yoon S., Langer N., 2005, *A&A*, 435, 967
- Yoon S., Podsiadlowski P., Rosswog S., 2007, *MNRAS*, 380, 933
- Yu S., Jeffery C. S., 2010, *A&A*, 521, A85+

Star	H	Li	C	N	O	F	Ne	Na	Mg	Al	Si	P	S	Ar	Ca	Ti	Cr	Fe	Ni	Zn	Y	Zr	Ba	La		
RCrB majority																										
R CrB	6.9	2.8	9.2	8.4	9.0	6.9		6.1	5.8	7.2		6.8		5.3		6.5	5.5		1.5		1.6					
RY Sgr	6.9		8.9	8.5	7.9	7.0		6.3	6.0	7.3		7.3		5.3	4.1	6.7	5.9	4.5	1.9	1.8	1.4	1.0				
XX Cam	4.1		9.0	8.9	8.4	<5.6		6.8		7.1		6.8		5.4	4.0	6.8	6.1		2.0		1.5					
SU Tau	7.4	2.6	8.8	8.5	8.4	7.0		5.6	5.2	6.7		6.5		5.0	3.7	6.1	5.4	3.6	1.3		0.3					
UX Ant	6.8		8.9	8.3	8.8	<6.2		5.8		6.9		6.2		5.5		6.2	5.8		1.5		1.0					
UV Cas	6.0		9.2	8.5	7.5	6.2		6.4	6.0	7.4		7.0		5.6	4.0	6.9	6.2	4.8	2.8		2.1	1.5				
UW Cen	6.5	3.5	8.6	8.3	7.7	7.1		6.0	5.7	6.3	7.0		6.7		5.2	4.1	6.3	5.9	4.3	1.5	1.8	1.6	1.5			
V482 Cyg	4.8		8.9	8.8	8.1	6.6		6.3	6.2	7.2		6.9		5.4		6.7	5.8	4.4	2.6	2.3	2.6	2.2				
Y Mus	6.1		8.9	8.8	7.7		8.3	6.3	6.3	6.1	7.3	5.9	6.9		5.3	4.2	6.5	6.0	4.4	2.4	2.6	1.5	1.3			
RT Nor	6.5		8.9	9.1	8.4			6.3	6.2	7.4		7.7		5.8		6.8	6.2	4.7	3.1	1.8	2.0	1.9				
RZ Nor	5.2	3.5	8.9	8.7	8.9			6.4	6.3	7.1		6.8		5.4		6.6	5.9	4.4	2.0		1.5	1.1				
FH Sct	5.6		8.8	8.7	7.7	7.2		6.1	5.9	7.1		7.0		5.1		6.3	5.8	4.1	2.0	2.3	1.6					
GU Sgr			8.8	8.7	8.2	7.2		6.0	6.9	5.7	7.2		7.0		5.4		6.3	5.6	4.4	2.4	1.2	0.8				
RS Tel	7.4		8.9	8.8	8.3			6.0	5.9	7.1		6.8		5.3		6.4	5.7	4.3	1.9		1.5					
RCrB minority																										
V3795 Sgr	4.1		8.8	8.0	7.5	6.7	7.9	5.9	6.1	5.6	7.5	6.5	7.4		5.3	3.5	5.6	5.8	4.1	1.3		0.9	0.5			
VZ Sgr	6.2		8.8	7.6	8.7	6.4		5.8		5.4	7.3		6.7		5.0		5.8	5.2	3.9	2.8	2.6	1.4				
V CrA	8.7	<0.9	8.8	8.0	7.8	6.5		5.7	6.6	5.4	7.6		7.2		5.2	3.3	5.5	4.9	3.9	1.1	1.4	0.3				
V854 Cen	9.9		9.6	7.8	8.9	<5.7		6.4	6.2	5.7	7.0		6.4		5.1	4.1	6.0	5.9	4.4	2.2	2.1	1.3	0.4			
EHe																										
LSS 3378	7.2		9.5	8.3	9.3	7.3		6.0	6.0	6.6	4.9	6.5			4.3	4.5	6.1			2.9	3.5	2.5				
BD+01°4381	6.2		9.0	7.2	8.9	6.5	8.1	5.4	6.0	4.7	6.1	4.2	6.0		4.2	3.2	3.6	5.4	4.0	3.2	2.1	1.0	0.6			
LS IV−14°109	6.1		8.9	8.6	8.5	6.5	8.9	6.4	7.0	7.0	7.2	5.8	7.1		5.6	4.0	6.3			1.9	1.9	1.7				
BD−01°3438	5.6		9.0	8.5	8.4	6.2	8.8	6.3	6.9	6.0	6.5	5.3	6.9		5.5	4.6	4.9	6.7								
LS IV−01°2	7.1		9.3	8.3	8.9	7.2	9.0	6.5	6.9	5.4	5.9	5.1	6.7		5.8	4.7	5.0	6.3	5.1		1.4	2.3				
HD 168476	<7.3		9.3	8.6	8.6	<7.2	7.6		7.8	6.2	7.0	6.1	7.2			5.2	5.1	7.0	5.7		2.9	3.1				
LSS 99	8.0		9.1	7.6	8.6				7.6	5.7	7.3	5.2	6.9	6.2	6.2		6.9									
MV Sgr			7.8	8.0							6.9	6.5														
HD 124448	<6.3		9.2	8.6	8.1		7.7		7.6	6.5	7.1	5.2	6.9	6.5	6.0	4.8	5.2	7.2	5.6		2.2	2.7				
LSS 4357	8.3		9.4	8.2	9.4				7.6	5.9	8.0	5.7	7.1	6.3	6.2		6.8									
LS II+33°5	<6.2		9.7	8.5	9.7		8.5		7.7	6.2	7.7	6.0	7.2	6.5	5.8	4.5	4.9	6.8	5.4	4.5	3.2	3.7		<2.2		
BD+10°2179	8.3		9.4	7.9	7.5		7.9		7.2	5.7	6.8	5.3	6.5	6.1	5.2	3.9	4.1	6.2	5.1	4.4	<1.4	<2.6				
LSE 78	<7.5		9.5	8.3	9.2		8.7		7.6	5.8	7.2	5.3	7.0	6.5	6.3	4.3	4.7	6.8	5.6	<4.4	<3.2	3.5		<3.2		
DY Cen	10.7		9.5	8.0	8.9		9.6		7.3	5.9	8.1	5.8	7.1	6.1			7.3									
BD−09°4395	8.7		9.2	8.0	7.9		8.2		7.3	5.6	7.8	6.2	7.8	7.2			6.6									
BX Cir	8.1		9.0	8.4	8.0				7.2	6.0	6.8	5.0	6.6				6.6									
LS IV+6°2	7.3		9.4	8.5	8.3		8.7		7.3	6.3	7.1	6.0	7.0				7.1									
HD 160641																										
Sun	12.0	1.2	8.6	8.1	8.0	4.6	8.1	6.3	7.6	6.5	7.6	5.5	7.2	6.6	6.4	5.0	5.7	7.5	6.3	4.6	2.2	2.6	2.1	1.2		

**Table 1.** Observed abundances for EHe and RCrB stars (omitting  $^{13}\text{C}/^{12}\text{C}$ ,  $^{18}\text{O}/^{16}\text{O}$ , Sc, Mn, Co, Cu, and Sr).